Electronic Supplementary Information

Toward fractioning of isomers through binding-induced acceleration of azobenzene switching

Rosaria Vulcano,[†] Paolo Pengo,[§] Simone Velari,[#] Johan Wouters,[†] Alessandro De Vita, [#,‡] Paolo Tecilla,[§] and Davide Bonifazi[¥,†,*]

[†]Department of Chemistry, University of Namur (UNamur), Rue de Bruxelles 61, Namur, 5000 (Belgium); [§]Department of Chemical and Pharmaceutical Sciences, University of Trieste, Piazzale Europa 1, Trieste, 34127 (Italy); [#]Department of Engineering and Architecture, University of Trieste, Piazzale Europa 1, Trieste, 34127 (Italy); [‡]Department of Physics, King's College London, Strand, London, WC2R 2LS (UK); [¥]School of Chemistry, Cardiff University, Main Building, Park Place, Cardiff, CF10 3AT (UK).

Table of contents

General remarks

Instrumentation

Preparative Thin Layer Chromatography (preparative TLC) were performed on SiO_2 pre-made glass backed plate prepared as follows: for fifteen 20 x 20 cm plates 440 g of silica gel 60 PF_{254} (Merck 107747) was shaken with 880 ml of phosphate buffer solution to obtain a free-flowing slurry. Using a *CAMAG 21602* automatic preparative spreader, the glass plates were covered with an even coating of adsorbent (1.5 mm). Just after coating, the plates are put down in a non-ventilated closed hood for 20 h. The dried plates are activated (140 °C, 10 h) prior use. **Melting points** (M.p.) were measured on a *Büchi Melting Point B-545* in open capillary tubes and have not been corrected. **Nuclear magnetic resonance** (NMR) ^{1}H, ^{13}C and ^{19}F spectra were obtained on a 270 MHz NMR (*Jeol JNM EX-270*) or 400 MHz (*Jeol JNM ECX-400*) or 500 MHz (*Jeol Resonance ECZ500R*) at rt otherwise stated. Chemical shifts were reported in ppm according to tetramethylsilane using the solvent residual signal as an internal reference ($CDCl_3$: δ_H = 7.26 ppm, δ_C = 77.16 ppm; CD_3CN: δ_H = 1.94, ppm, δ_C = 1.32 ppm; DMSO-d_6: δ_H = 2.50 ppm, δ_C = 39.52; toluene-d_8: δ_H = 2.08 ppm, δ_C = 20.43). Coupling constants (*J*) were given in Hz. Resonance multiplicity was described as *s* (singlet), *d* (doublet), *t* (triplet), *dd* (doublet of doublets), *dt* (doublet of triplets), *td* (triplet of doublets), *q* (quartet), *m* (multiplet) and *broad* (broad signal). Carbon spectra were acquired with a complete decoupling for the proton. **Infrared spectra** (IR) were recorded on a *Perkin-Elmer Spectrum II FT-IR System* with *Specac* Silver Gate Evolution single-reflection ATR mounted with a diamond mono-crystal. **High-resolution mass spectrometry** (HRMS) measurements were generally performed by the "Fédération de Recherche" ICOA/CBM (FR2708) platform of Orléans in France. High-resolution ESI mass spectra (HRMS) were performed on a *Bruker maXis Q-TOF* in the positive ion mode. The analytes were dissolved in a suitable solvent at a concentration of 1 mg/mL and diluted 200 times in methanol (≈ 5 ng/mL). The diluted solutions (1μL) were delivered to the ESI source by a Dionex Ultimate 3000 RSLC chain used in FIA (Flow Injection Analysis) mode at a flow rate of 200 μL/min with a mixture of CH_3CN/H_2O+0.1% of HCO_2H (65/35). ESI conditions were as follows: capillary voltage was set at 4.5 kV; dry nitrogen was used as nebulizing gas at 0.6 bars and as drying gas set at 200°C and 7.0 L/min. ESI-MS spectra were recorded at 1 Hz in the range of 50-3000 *m/z*. Calibration was performed with ESI-TOF Tuning mix from Agilent and corrected using lock masses at *m/z* 299.294457 (methyl stearate) and 1221.990638 (HP-1221). Data were processed using *Bruker DataAnalysis 4.*1 software. **Liquid chromatography mass**

spectrometry (LC-HRMS) measurements were conducted on an *Agilent 6210 series TOF mass spectrometer* equipped with ESI and APCI ionization sources and a Time Of Flight (TOF) detector, operating in positive mode. The analyte solutions were delivered to the ESI or APCI source by an *Agilent 1200 series LC system* at a flow rate of 0.25 mL/min. Typical elution gradient start from H_2O (90%) to CH_3CN (100%) for 20 minutes. ESI mode: Typical ESI conditions were capillary voltage 2.0 kV; cone voltage 65 V; source temperature 150 °C; desolvation temperature 250 °C; drying gas 5 L/min, nebulizer 60 psig. APCI: Typical APCI conditions were, capillary voltage 2.0 kV; cone voltage 65 V; source temperature 250 °C; desolvation temperature 350°C; drying gas 5L/min; nebuliser 60 psig. Dry nitrogen was used as the ESI and APCI gas. Data were processed using *Mass Hunter* software. **High-resolution Electron Ionization mass spectrometry** (EI-HRMS) measurements were performed by the "Groupe de Recherche en Spectrométrie de Masse" GRSM/ZMa of Mons in Belgium. High-resolution electron ionization mass spectra (EI-HRMS) were performed on a *Waters Autospec 6F*. **UV/Vis absorption spectra** were recorded with a V*arian Cary 5000 UV-Vis-NIR* spectrophotometer, using quartz cells with path length of 1.0 cm. All photophysical experiments were carried out in air-equilibrated solutions at 25 °C otherwise stated. **Light irradiation** experiments were performed with monochromatic light produced with a *LOT Oriel* equipment, consisting of a 1000 W Xe lamp (*LSB551* ozone free) connected via an axial optical path to a computer controlled monochromator *MSH-300*. The 180° optical path was composed of a condenser lens, which collimated the light emitted from the source, and a focusing lens aligned to the monochromator entrance slit. The entrance and the exit slits of the monochromator were adjusted in order to have a 20 nm bandwidth output light. The sample was placed in the collimated beam of the monochromatic light. **X-ray** measurements were performed on a *Gemini Ultra R system* (4-circle kappa platform, Ruby CCD detector) using Mo Kα radiation (λ = 0.71073 Å) or Cu Kα radiation (λ = 1.54178 Å) at Université de Namur (UNamur) in Belgium. After mounting and centering of the single crystal on the diffractometer, cell parameters were estimated from a pre-experiment run and full data sets collected at room temperature. Structures were solved by direct methods with SHELXS-86 program and then refined on F^2 using SHELXL-97 software.[1] Non-hydrogen atoms were anisotropically refined.

Materials and general methods

Synthesis. Chemicals were purchased from *Sigma Aldrich*, *Acros Organics*, *TCI* and *ABCR* and used as received. Solvents were purchased from *Sigma Aldrich*, except for deuterated

solvents from *Eurisotop,* and anhydrous DMF from *Acros Organics*. Anhydrous THF and CH_2Cl_2 were distilled from Na/benzophenone and P_2O_5 respectively. Toluene-d_8 for NMR studies was dried over molecular sieves. Low temperature baths from -15 °C to -20 °C were prepared with crushed ice and solid NaCl, those at -84 °C with AcOEt/ liquid N_2. Anhydrous conditions were achieved by flaming the glassware (Schlenk tubes or two neck round bottom flasks) with a heat gun under vacuum and then purging them with Argon. The dry and inert atmosphere was maintained using Argon-filled balloons equipped with a syringe and needle that was used to penetrate the silicon stoppers used to close the flasks' necks. Additions of liquid reagents were performed using dried plastic or glass syringes.

Determination of the binding stoichiometry by Job's plot analysis. The binding stoichiometry of the HOST-GUEST complexes was determined as it follows. Two stock solutions were prepared, solution A containing 3.0 mM of HOST in toluene-d_8 ($[H]_0$) and solution B containing the same concentration of DAP in toluene-d_8 ($[G]_0$). Then, nine NMR tubes were filled with solutions A and B in the following volume ratios A:B (maximum volume 500 μL): 50:450, 100:400, 150:350, 250:250, 300:200, 350:150, 400:100, 450:50 and 500:0 μL. ^{1}H-NMR were recorded on a 500 MHz NMR (*Jeol Resonance ECZ500R*) at 25 °C, for each mixture and then the complex concentration (**[HG]**) defined by *Equation 1* plotted against the HOST molar fraction $\boldsymbol{x}_{\mathbf{H}}$.

$$[\mathrm{HG}] = [\mathrm{H}]_0 \cdot \frac{\Delta\delta}{\Delta\delta sat} \qquad \text{[Eq. 1]}$$

The observed change in chemical shift (Δδ) of the HOST signals is defined as the absolute difference between the chemical shift observed at a given HOST-GUEST complex concentration and the chemical shift of the free host. The difference in chemical shift at saturation is expressed by Δδsat. The HOST molar fraction (is defined by *Equation 2*:

$$x_{\mathrm{H}} = \frac{[\mathrm{H}]_0}{[\mathrm{H}]_0 + [\mathrm{G}]_0} \qquad \text{[Eq. 2]}$$

^{1}H-NMR titrations. ^{1}H-NMR spectra were obtained on a 500 MHz NMR (*Jeol Resonance ECZ500R*) at 25 °C. Titrations were performed with multiple additions of the GUEST solution (DAP, around 15 mM concentration) in 0.5 mL of the HOST solution (uracil derivatives Upr and 5AUP, around 3 mM concentration), using standard NMR tubes and keeping the samples in the dark. For the *Z*-5AUP titration, the HOST solution was introduced in a quartz NMR tube and the sample was irradiated for 50 min at 360 nm before the NMR analysis and the additions. HOST samples were prepared dissolving uracil derivatives in toluene-d_8, GUEST samples were prepared dissolving 2,6-diacetylamino-4-[(trimethylsilyl)ethynyl]pyridine (DAP) in the HOST solution, except for the *Z*-5AUP

titration were the GUEST was dissolved in toluene-d_8. The chemical shift data of the imide protons were fitted against GUEST concentration using *Dynafit* software package.[2] The formation constant for the complexes are the average values of few independent experiments with consistent results, otherwise discharged. The stoichiometry of the different complexes was established by Job's plot experiments. The dimerization constants were established by ^{1}H-NMR dilution experiments of 5 mM HOST solution in toluene-d_8 at 25 °C, in all cases the values obtained were lower than 100 M^{-1}, small enough to neglect the interference of the dimerization process on the binding events.

^{1}H-NMR kinetic studies. ^{1}H-NMR spectra were obtained on a 500 MHz NMR (*Jeol Resonance ECZ500R*) at 25 °C. The sample was introduced in a quartz NMR tube and irradiated at 360 nm for 40 min before the NMR analysis. The sample was kept in the NMR instrument with the probe at 25 °C for all the experiment duration. Isomers concentrations were calculated on the integrals of the peaks area corresponding to the N-H imide protons or to the N-CH_2 methylene protons for both isomers, depending on the resolution of those signals.

UV-Vis kinetic studies. UV/Vis absorption spectra were recorded with a V*arian Cary 5000 UV-Vis-NIR* spectrophotometer at 25 °C. The samples solutions were introduced in quartz cells with path length of 1.0 cm and irradiated at λ_{max} for 40 min before starting the kinetic studies. The extinction coefficients were determined in prior experiments.

DFT calculations. DFT calculations were performed using the ab initio pseudopotential plane-wave method as implemented in the PWSCF code of the Quantum ESPRESSO distribution,[3] using Ultrasoft pseudopotentials from the publicly available repository.[4] For the exchange-correlation term, a GGA-PBE approximation has been used.[5] The valence electronic wave functions were expanded onto a plane wave basis set with a kinetic energy cutoff of 408 eV. The Brillouin zone integration for the gas-phase systems investigated has been limited to the Γ-point only. Since van der Waals interactions play a non-negligible role in this system, we adopted the VdW-DF functional developed by Langreth and coworkers,[6][7][8] implemented in the QE package, which uses a very efficient FFT formulation.[9] Ball and stick models are rendered using the XCrySDen software.[10]

Synthetic procedures and spectral data

2,6-Diacetylamino-4-[(trimethylsilyl)ethynyl]pyridine and 6-chlorouracil were prepared according to literature procedure.[11,12]

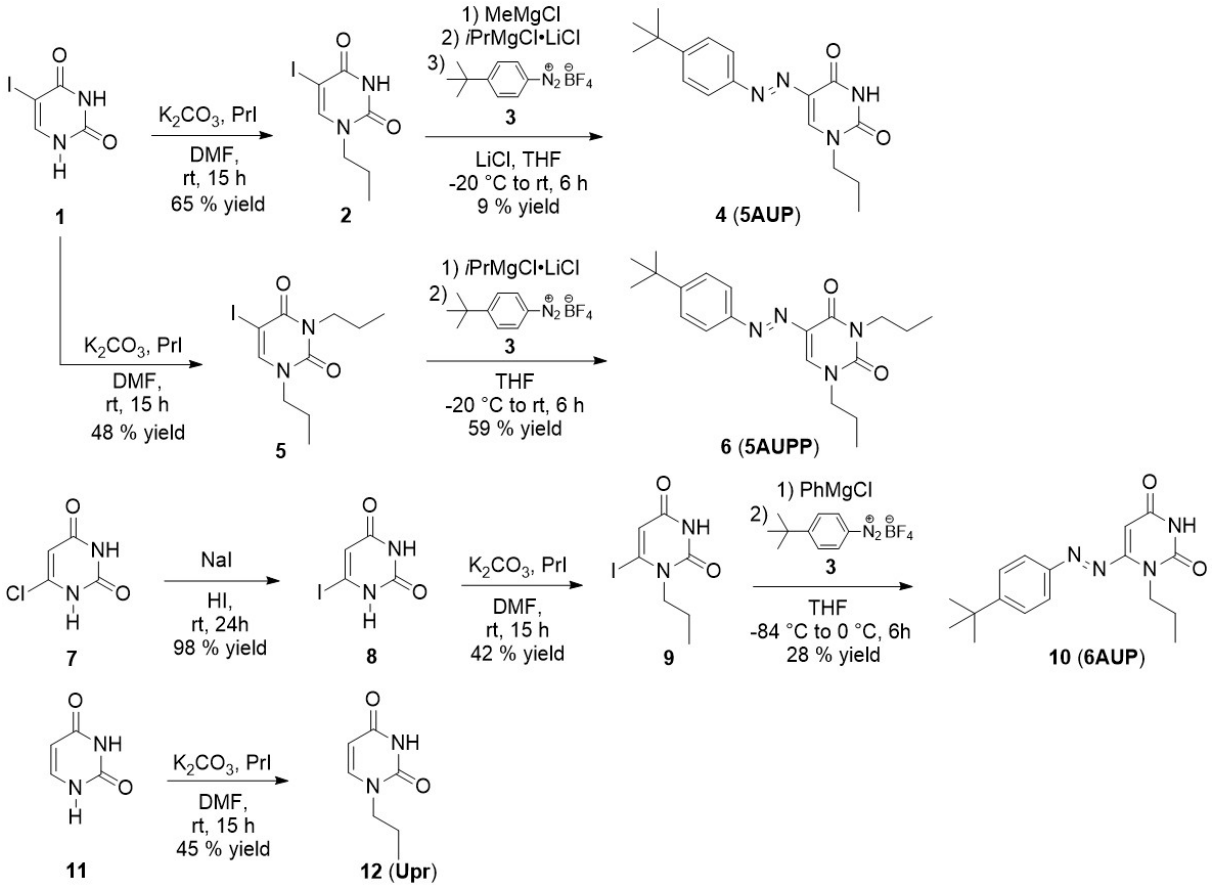

Synthesis of 4-*tert*-butylbenzenediazonium tetrafluoroborate.[13] (3)

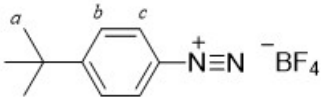

A solution of *tert*-buthylaniline (1.7907 g, 12 mmol) in dry CH_2Cl_2 (24 mL) was added to $BF_3{\cdot}Et_2O$ (2.5547 g, 18 mmol) at -15 °C under Ar, followed by the dropwise addition of a solution of *tert*-buthylnitrite (90 % wt, 1.4849 g, 14 mmol) in dry CH_2Cl_2 (12 mL). The reaction mixture was stirred for 10 min at -15 °C, before allowing the temperature to increase to rt over 2 h 30 min. The resulting violet mixture was added dropwise to 50 mL of cold Et_2O. The precipitate was filtered under reduced pressure and washed with cold Et_2O (3 x 5 mL) to afford pure compound **3** as white powder (2.8348 g, 95 % yield). $C_{10}H_{13}BF_4N_2$, MW: 248.04 g/mol. M.p.: 84 °C (dec.). IR ν_{max} (KBr) (cm^{-1}): 3428, 3089, 2968, 2265 (N≡N), 1641, 1578, 1478, 1416, 1369, 1304, 1078, 844, 537. ^{1}H-NMR ($CDCl_3$, 400 MHz) δ: 8.56 (d, J = 9.0 Hz, 2H, H_c), 7.81 (d, J = 9.0 Hz, 2H, H_b), 1.35 (s, 9H, H_a). ^{13}C-NMR ($CDCl_3$, 100 MHz) δ: 167.4, 132.9, 129.1, 110.5, 36.9, 30.6. 19F-NMR (CDCl3, 376 MHz) δ: -149.19. All characterizations are in full agreement with the previously reported in the literature.[14][15]

Synthesis of 5-iodo-2,4-dioxo-1-propyl-3-hydropyrimidine. (2)

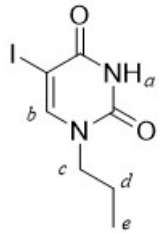

To a solution of 5-iodouracil (**1**, 2.400 g, 10 mmol) in dry DMF (50 mL) was added K_2CO_3 (0.6010 g, 4.3 mmol) and the resulting mixture was stirred at rt for 15 min under Ar. After the addition of iodopropane (0.7310 g, 4.3 mmol) the mixture was stirred for further 15 h at rt under Ar. The reaction was quenched with 10 ml of H_2O. AcOEt (50 ml) was added to the mixture and the two phases were separated. The aqueous phase was acidified to pH 5 by dropwise addition of HCl 1 M solution before the extraction with AcOEt (7 x 20 ml). The combined organic layers were dried over Na_2SO_4 and solvents removed under reduced pressure. The crude was purified by column chromatography (silica gel, CH_2Cl_2/AcOEt 9/1) to afford pure compound **2** as white powder (0.7815 g, 65 % yield). $C_7H_9IN_2O_2$. MW: 280.07 g/mol. M.p.: 189 °C. IR ν_{max} (cm^{-1}): 3158, 3029, 2990, 2871, 1693, 1644, 1602, 1441, 1413, 1328, 1240, 1158, 1026, 854, 755, 616, 534, 456. ^{1}H-NMR ($CDCl_3$, 400 MHz) δ: 8.39 (bs, 1H, H_a), 7.61 (s, 1H, H_b), 3.71 (m, 2H, H_c), 1.73 (m, 2H, H_d), 0.97 (t, J = 7.6 Hz, 3H, H_e). ^{13}C-NMR ($CDCl_3$, 100 MHz) δ: 160.3, 150.3, 149.1, 67.5, 50.9, 22.6, 11.0. LC-HRMS (ESI-): $[M-H]^-$ calc. 278.9636, found 278.9618.

Synthesis of 5-((4-(*tert*-butyl)phenyl)diazenyl)-1-propylpyrimidine-2,4(3H)-dione. (4, 5AUP)

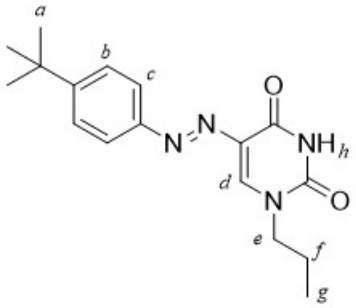

A solution of LiCl in dry THF (0.5 M, 4 mL, 2 mmol)[16] was added to 5-iodo-2,4-dioxo-1-propyl-3-hydropyrimidine (**2**, 0.5610 g, 2 mmol). The resulting solution was cooled at -20 °C before the dropwise addition of a MeMgCl solution (22 % wt in dry THF, 0.67 mL, 2 mmol). After the end of the CH_4 bubbling, the mixture was stirred for further 20 min at -20 °C. A

solution of *i*PrMgCl·LiCl (1.3 M in dry THF, 1.85 mL, 2.4 mmol) was added to the mixture and allowed to warm up to rt stirring over 2 h. The resulting mixture was then cooled down to -20 °C before the dropwise addition of a solution of 4-*tert*-butylbenzenediazonium tetrafluoroborate (**3**, 0.5953 g, 2.4 mmol) in dry THF (20 mL). The reaction mixture was allowed to warm up to rt stirring over 4 h 30 min and quenched with 10 mL of H_2O. The two layers were separated and the aqueous phase was extracted with AcOEt (3 x10 mL). The combined organic layers were dried over $MgSO_4$ and solvents removed under reduced pressure. The crude was purified by column chromatography (silica gel, CH_2Cl_2/AcOEt 9/1) affording compound **4** as sticky red oil. Further precipitation from Et_2O (5 mL) upon addition of toluene (1 mL) afforded pure compound **4** as orange powder (57.8 mg, 9 % yield). $C_{17}H_{22}N_4O_2$. MW: 314.39 g/mol. M.p.: 195-197 °C. IR ν_{max} (cm^{-1}): 2963, 1707, 1668, 1600, 1579, 1465 (N=N), 1442, 1421, 1364, 1337, 1240, 1102, 832, 819, 798, 755, 592, 563, 542, 502. ^{1}H-NMR (CD_3CN, 400 MHz) δ: 9.24 (bs, 1H, H_h), 8.02 (s, 1H, H_d), 7.71 (d, J = 8.8 Hz, 2H, H_c), 7.56 (d, J = 8.8 Hz, 2H, H_b), 3.76 (m, 2H, H_e), 1.73 (m, 2H, H_f), 1.35 (s, 9H, H_a), 0.94 (t, J = 7.4 Hz, 3H, H_g). ^{13}C-NMR (CD_3CN, 100 MHz) δ: 161.0, 155.6, 151.5, 151.1, 137.6, 130.2, 127.3, 123.1, 51.5, 35.6, 31.4, 23.0, 11.1. LC-HRMS (ESI+): $[M+H]^+$ calc. 315.1821, found 315.1874. UV-Vis (toluene, 25 °C) λ_{max} (ε, $Lmol^{-1}cm^{-1}$): 360 nm (20727). Crystals obtained by slow evaporation of toluene solution, space group: P21/n.

Synthesis of 5-iodo-2,4-dioxo-1,3-dipropylpyrimidine. (5)

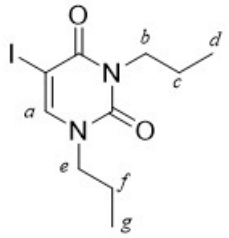

To a solution of 5-iodouracil (**1**, 1.1899 g, 5 mmol) in dry DMF (25 mL) was added K_2CO_3 (0.6911 g, 5 mmol) and the resulting mixture was stirred at rt for 15 min under Ar. After the addition of iodopropane (1.8152 g, 11 mmol) the mixture was stirred for further 15 h at rt under Ar. The reaction was quenched with 10 ml of H_2O. AcOEt (50 mL) was added to the mixture and the two phases were separated. The aqueous phase was acidified to pH 5 by dropwise addition of HCl 1 M solution before the extraction with AcOEt (7 x 20 mL). The combined organic layers were dried over Na_2SO_4 and solvents removed under reduced pressure. The crude was purified by column chromatography (silica gel, CH_2Cl_2/AcOEt 9/1) to afford pure compound **5** as white powder (0.7672 g, 48 % yield). $C_{10}H_{15}IN_2O_2$. MW:

322.15 g/mol. M.p.: 91 °C. IR ν_{max} (cm^{-1}): 2967, 1696, 1650, 1637, 1612, 1434, 1421, 1377, 1356, 1301, 1240, 1204, 1053, 926, 764, 752, 607, 548, 466. ^{1}H-NMR ($CDCl_3$, 400 MHz) δ: 7.59 (s, 1H, H_a), 3.95 (m, 2H, H_b), 3.71 (m, 2H, H_e), 1.66 (m, 4H, $H_{c,f}$), 0.95 (m, 6H, $H_{d,g}$). ^{13}C-NMR ($CDCl_3$, 100 MHz) δ: 160.2, 151.1, 147.0, 67.7, 51.8, 44.7, 22.6, 20.9, 11.4, 10.0. HRMS (ESI+): $[M+H]^+$ calc. 323.0251, found 323.0249; $[M+Na]^+$ calc. 345.0070, found 345.0069.

Synthesis of 5-((4-(*tert*-butyl)phenyl)diazenyl)-1,3-dipropylpyrimidine-2,4-dione. (6, 5AUPP)

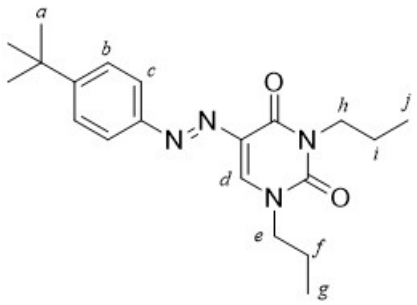

A solution of 5-iodo-2,4-dioxo-1,3-dipropylpyrimidine (**5**, 96.6 mg, 0.3 mmol) in dry THF (1 mL) was cooled at -20 °C before the dropwise addition of *i*PrMgCl·LiCl (1.3 M in THF, 0.25 mL, 0.33 mmol). The resulting mixture was stirred under Ar allowing the temperature to increase to rt over 2 h. A solution of 4-*tert*-butylbenzenediazonium tetrafluoroborate (**3**, 96.7 mg, 0.39 mmol) in dry THF (6 mL) was added dropwise to the reaction mixture and stirred for further 4 h allowing the temperature to increase to rt. The reaction was quenched with H_2O (10 mL) and the two layers separated. The aqueous phase was extracted with AcOEt (3 x 20 mL), the combined organic layers were dried over $MgSO_4$ and solvents removed under reduced pressure. The crude was purified by preparative TLC (silica gel, CH_2Cl_2/AcOEt 95/5) affording pure compound **6** as red oil (63.4 mg, 59 % yield). $C_{20}H_{28}N_4O_2$. MW: 356.47 g/mol. IR ν_{max} (cm^{-1}): 2962, 2907, 2875, 1711, 1662, 1610, 1499, 1458 (N=N), 1380, 1363, 1334, 1267, 1232, 1163, 1105, 844, 775, 758, 566, 498. ^{1}H-NMR ($CDCl_3$, 400 MHz) δ: 7.91 (s, 1H, H_d), 7.80 (d, J = 8.4 Hz, 2H, H_c), 7.49 (d, J = 8.4 Hz, 2H, H_b), 4.05 (m, 2H, H_h), 3.85 (m, 2H, H_e), 1.77 (m, 4H, $H_{f,i}$), 1.35 (s, 9H, H_a), 1,00 (m, 6H, $H_{g,j}$). ^{13}C-NMR ($CDCl_3$, 126 MHz) δ: 160.2, 154.9, 150.7, 150.5, 132.7, 129.0, 126.1 122.8, 52.2, 43.5, 35.1, 31.3, 22.6, 21.0, 11.5, 11.1. HRMS (ESI+): $[M+H]^+$ calc. 357.2285, found 357.2282. UV-Vis (toluene, 25 °C) λ_{max} (ε, $Lmol^{-1}cm^{-1}$): 364 nm (12561).

Synthesis of 6-iodo-2,4-dioxo-1,3-dihydropyrimidine.[17] (8)

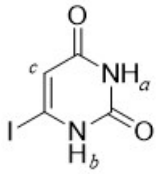

To a solution of 6-chlorouracil (**7**, 1.3189 g, 9 mmol) in HI (57 %, 24 mL) was added NaI (6.745 g, 45 mmol). The reaction mixture was stirred at rt for 24 h before filtering it under reduced pressure. The solid obtained was washed with cold CH_3CN (3 x 5 mL) followed by cold Et_2O (3 x 5mL), and finally dried under high vacuum to afford pure compound **8** as pale yellow powder (2.100 g, 98 % yield). $C_4H_3IN_2O_2$. MW: 237.98 g/mol. M.p.: 250 °C (dec.). ^{1}H-NMR (DMSO-d_6, 400 MHz) δ: 11.57 (s, 1H, H_a), 11.19 (s, 1H, H_b), 6.01 (s, 1H, H_c). ^{13}C-NMR (DMSO-d_6, 100 MHz) δ: 162.97, 151.12, 111.71, 110.62. All characterizations are in full agreement with the previously reported in the literature.[17,18]

Synthesis of 6-iodo-2,4-dioxo-1-propyl-3-hydropyrimidine. (9)

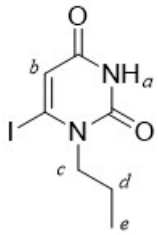

To a solution of 6-iodo-2,4-dioxo-1,3-dihydropyrimidine (**8**, 1.3267 g, 5.6 mmol) in dry DMF (80 mL), was added K_2CO_3 (0.2764 g, 2 mmol). The mixture was stirred under Ar at rt for 15 min, before the addition of iodopropane (0.2 mL, 2 mmol). The reaction was stirred for further 15 h at rt, under Ar and the solvent removed under reduced pressure. The crude mixture was taken up in H_2O (10 mL), followed by addition of AcOEt (20 mL). The two phases were separated, the aqueous phase acidified to pH 5 by dropwise addition of HCl 1 M solution and extracted with AcOEt (7 x 20 mL). Combined organic layers are washed with H_2O (5 mL) and brine (10 mL), dried over Na_2SO_4 and solvent removed under reduced pressure. The crude was purified by column chromatography (silica gel, CH_2Cl_2/AcOEt 9/1) to afford pure compound **9** as light yellow powder (0.2334 g, 42 % yield). $C_7H_9IN_2O_2$. MW: 280.07 g/mol. M.p.: 168 °C. IR ν_{max} (cm^{-1}): 3159, 3029, 2955, 2866, 1660, 1558, 1429, 1392, 1348, 1312, 1166, 1060, 997, 825, 786, 750, 638, 573, 558, 533. ^{1}H-NMR ($CDCl_3$, 400 MHz) δ: 8.48 (s, 1H, H_a), 6.41 (s, 1H, H_b), 4.03 (m, 2H, H_c), 1.72 (m, 2H, H_d), 0.98 (t, J = 7.6 Hz,

3H, H_e). ^{13}C-NMR ($CDCl_3$, 68 MHz) δ: 161.2, 148.1, 115.8, 113.9, 55.1, 22.3, 10.8. HRMS (ESI +): $[M+H]^+$ calc. 280.9782, found 280.9777; $[M+Na]^+$ calc. 302.9601, found 302.9598.

Synthesis of 6-((4-(tert-butyl)phenyl)diazenyl)-2,4-dioxo-1-propyl-3-hydropyrimidine. (10, 6AUP)

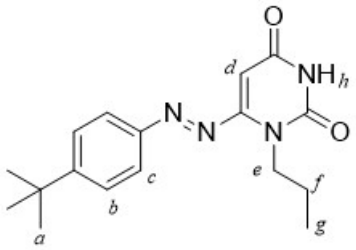

A solution of 6-iodo-2,4-dioxo-1-propyl-3-hydropyrimidine (**9**, 42.0 mg, 0.15 mmol) in dry THF (3 mL) was cooled at -84 °C and stirred 30 min before the dropwise addition of PhMgCl (2.0 M in toluene, 0.15 mL, 0.30 mmol). The reaction mixture was further stirred at -84 °C for 1 h before the dropwise addition of the solution of 4-tert-butylbenzenediazonium tetrafluoroborate (**3**, 44.6 mg, 0.18 mmol) in dry THF (3 mL). The mixture was stirred for further 4 h 30 min allowing the temperature to increase to 0 °C. The reaction was quenched with H_2O, the two layers separated, and the aqueous phase neutralized by dropwise addition of a saturated solution of NH_4Cl. The aqueous phase was extracted with AcOEt (3 x 20 mL), combined organic layers were dried over $MgSO_4$, and solvents removed under reduced pressure. The crude was purified by preparative TLC (cyclohexane/AcOEt 7/3) to afford pure compound **10** as orange powder (13.0 mg, 28 % yield). $C_{17}H_{22}N_4O_2$. MW: 314.39 g/mol. M.p.: 179 °C. IR ν_{max} (cm^{-1}): 3170, 3047, 2959, 2871, 1692, 1667, 1599, 1441 (N=N), 1408, 1364, 1341, 1101, 1028, 850, 828, 575, 554, 524. ^{1}H-NMR ($CDCl_3$, 400 MHz) δ: 8.19 (s, 1H, H_h), 7.86 (d, J = 8.6 Hz, 2H, H_c), 7.60 (d, J = 8.6 Hz, 2H, H_b), 5.74 (s, 1H, H_d), 4.16 (m, 2H, H_e), 1.74 (m, 2H, H_f), 1.39 (s, 9H, H_a), 0.95 (t, J = 7.4 Hz, 3H, H_g). ^{13}C-NMR ($CDCl_3$, 100 MHz) δ: 163.1, 159.3, 158.9, 150.9, 150.4, 126.8, 124.5, 87.1, 44.9, 35.6, 31.2, 22.8, 11.3. EI-HRMS: $[M]^+$ calc. 314.1743, found 314.1754. UV-Vis (toluene, 25 °C) λ_{max} (ε, $Lmol^{-1}cm^{-1}$): 329 nm (24111). Crystals obtained by slow evaporation of toluene solution, space group: P-1.

Synthesis of 2,4-dioxo-1-propyl-3-hydropyrimidine. (12, Upr)

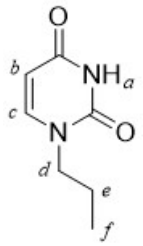

To a solution of Uracil (**11**, 0.5 g, 4.5 mmol) in dry DMF (63 mL) were added K_2CO_3 (0.6 g, 4.5 mmol) and iodopropane (0.44 mL, 4.5 mmol). The reaction mixture was stirred under Ar at rt for 24 h. The reaction was quenched with a saturated solution of NH_4Cl (10 mL) and extracted with AcOEt (3 x 15 mL). The combined organic layers were washed with brine (2 mL), dried over Na_2SO_4 and solvent removed under reduced pressure. The crude was purified by column chromatography (silica gel, CH_2Cl_2/EtOH 95/5) to afford pure compound **12** as white powder (0.3093 g, 45 % yield). $C_7H_{10}N_2O_2$. MW: 154.17 g/mol. M.p.: 112-115 °C. IR ν_{max} (cm^{-1}): 3039, 1622, 1456, 1353, 1247, 806, 759, 722, 546. ^{1}H-NMR ($CDCl_3$, 400 MHz) δ: 8.27 (s, 1H, H_a), 7.15 (d, J = 8.0 Hz, 1H, H_c), 5.69 (dd, J = 8.0, 2.4 Hz, 1H, H_b), 3.69 (m, 2H, H_d), 1.73 (m, 2H, H_e), 0.97 (t, J = 7.2 Hz, 3H, H_f). ^{13}C-NMR ($CDCl_3$, 68 MHz) δ: 161.7, 150.9, 144.6, 102.2, 50.6, 22.5, 11.0. HRMS (ESI +): $[M+H]^+$ calc. 155.0815, found 155.0818; $[M+Na]^+$ calc. 177.0634, found 177.0637. Crystals obtained by slow evaporation of CH_3CN solution, space group: P21/n. All characterizations are in full agreement with the previously reported in the literature.[19]

^{1}H and ^{13}C NMR spectra

5-iodo-2,4-dioxo-1-propyl-3-hydropyrimidine. (2)

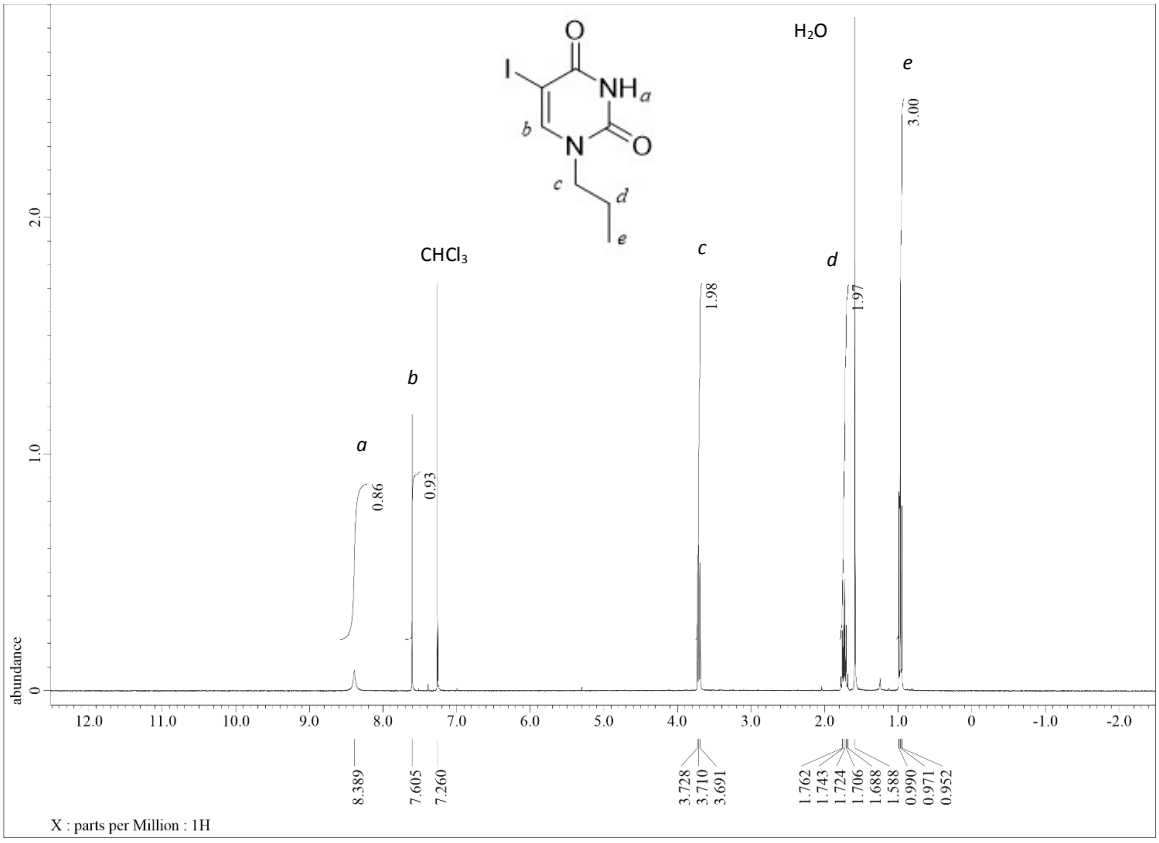

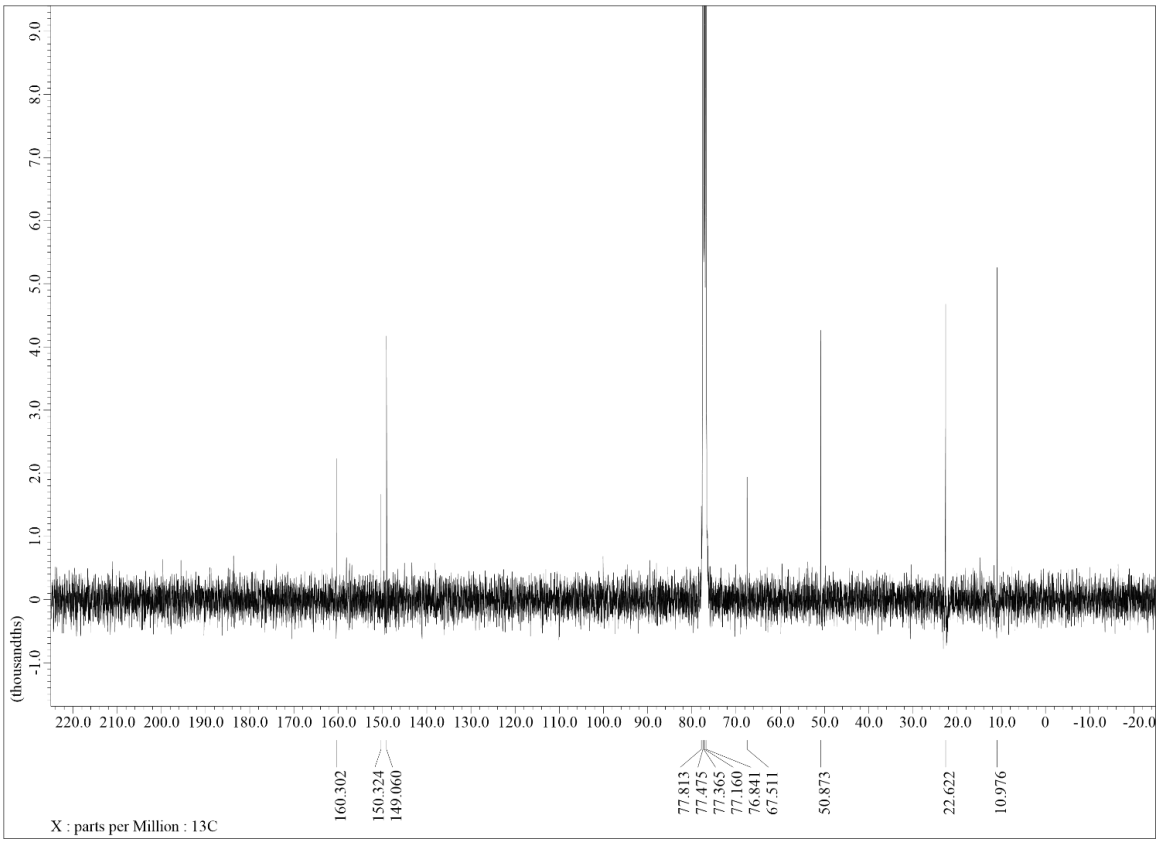

5-((4-(*tert*-butyl)phenyl)diazenyl)-2,4-dioxo-1-propyl-3-hydropyrimidine (4, 5AUP)

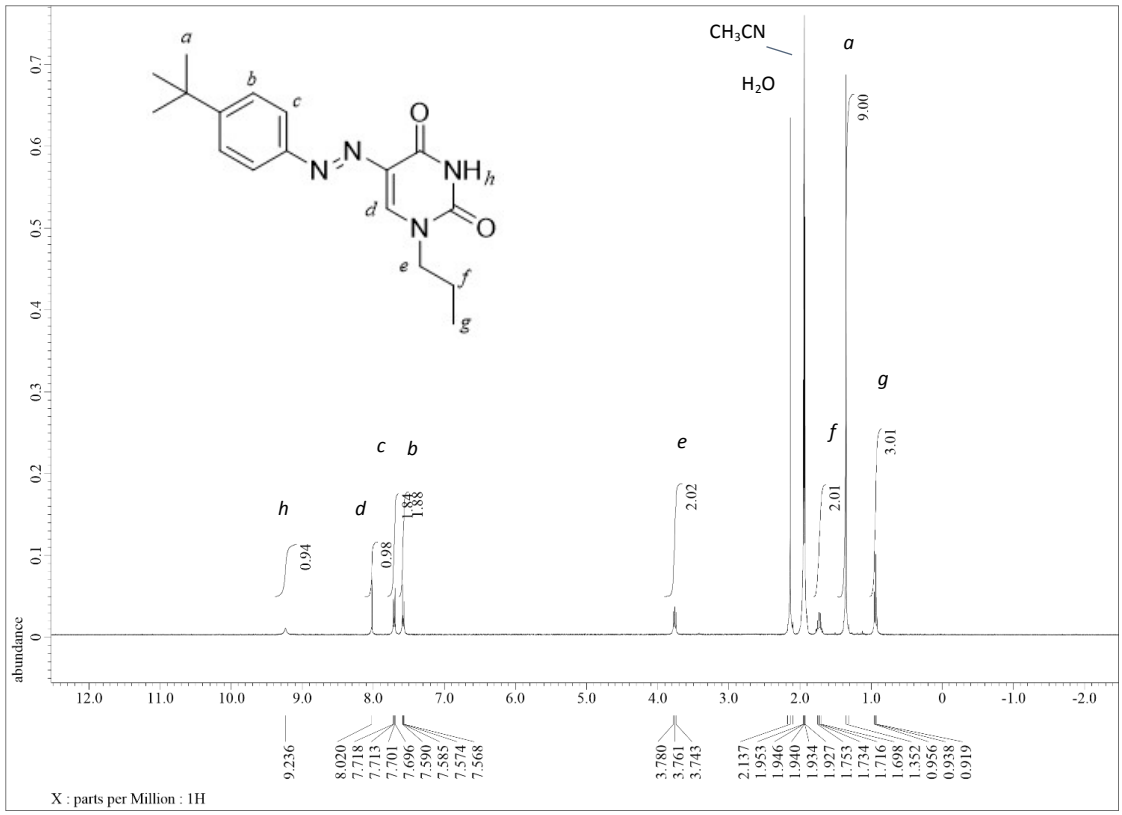

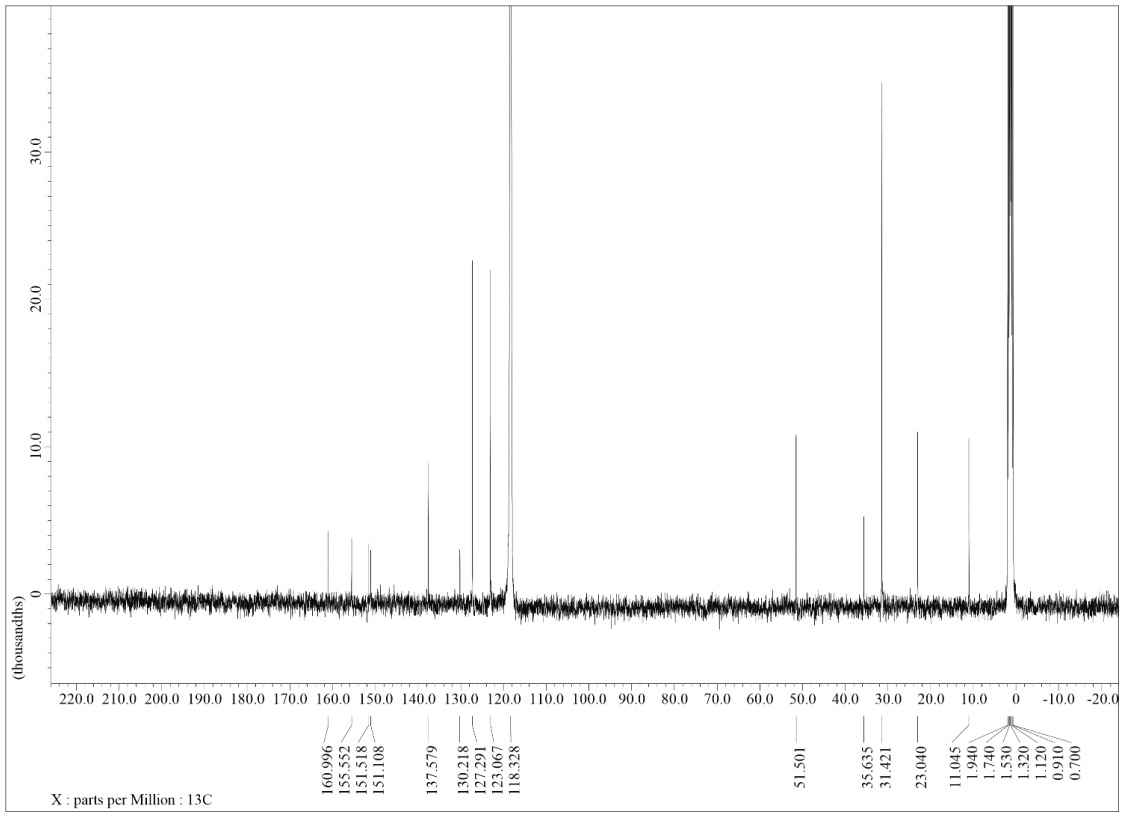

5-iodo-2,4-dioxo-1,3-dipropylpyrimidine. (5)

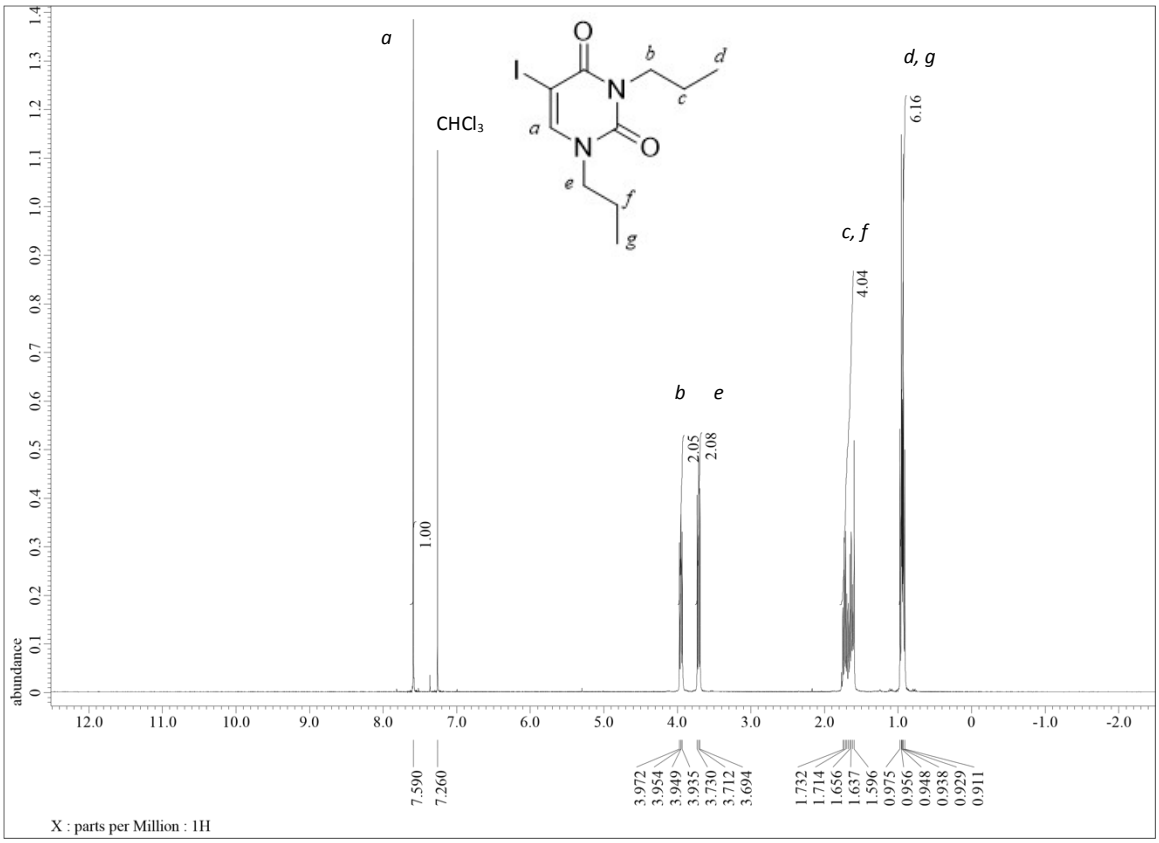

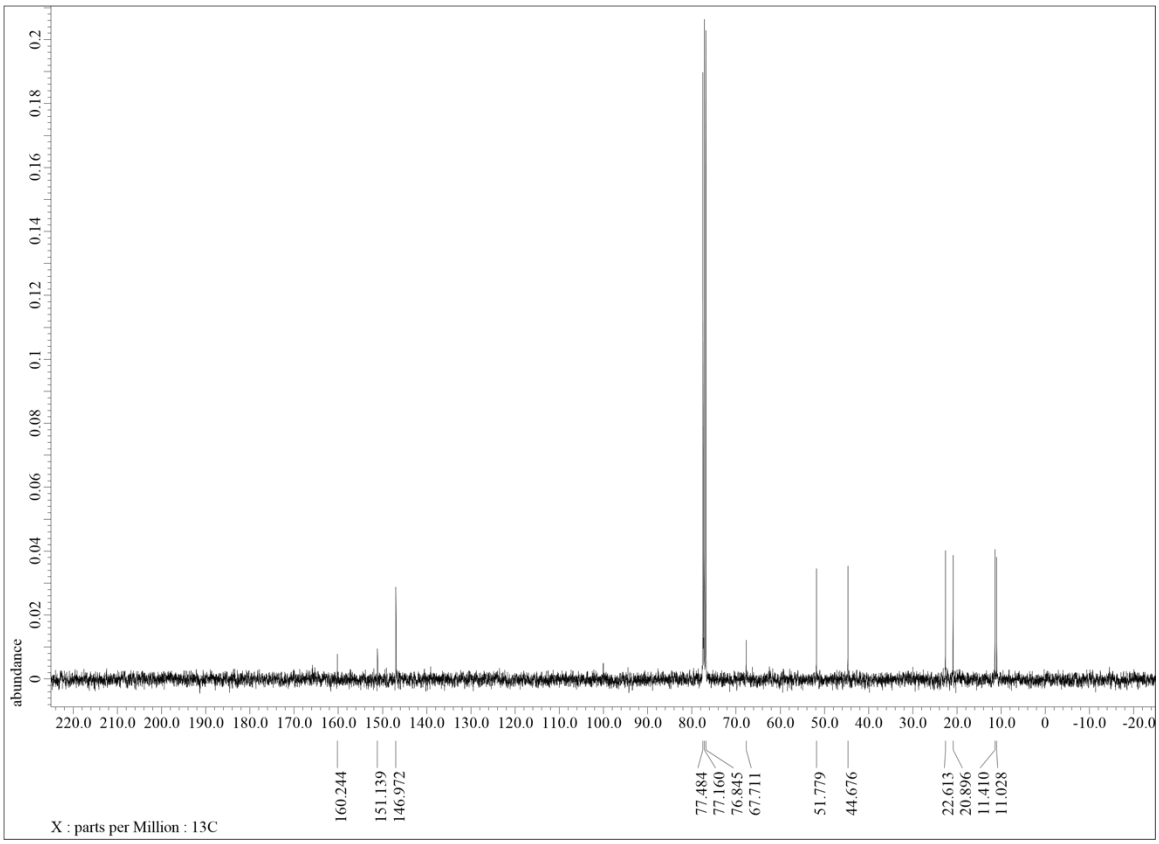

5-((4-(*tert*-butyl)phenyl)diazenyl)-2,4-dioxo-1,3-dipropylpyrimidine (6, 5AUPP)

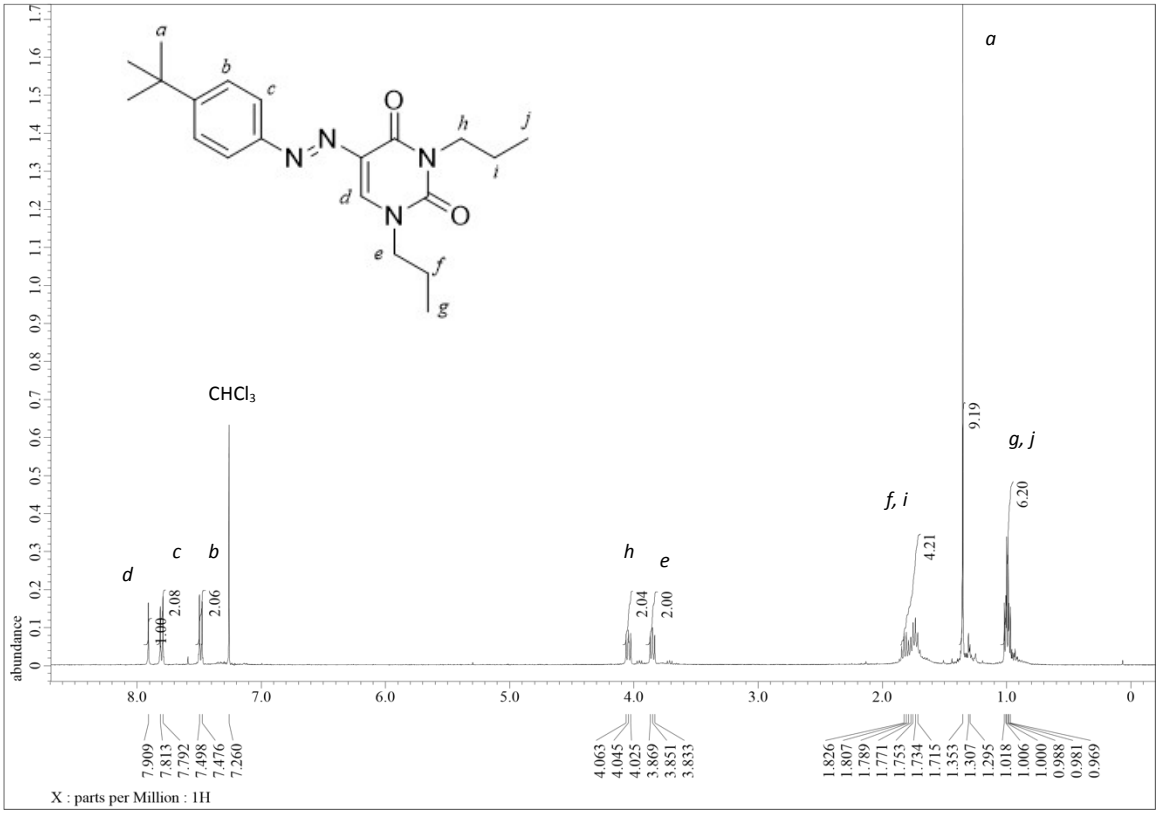

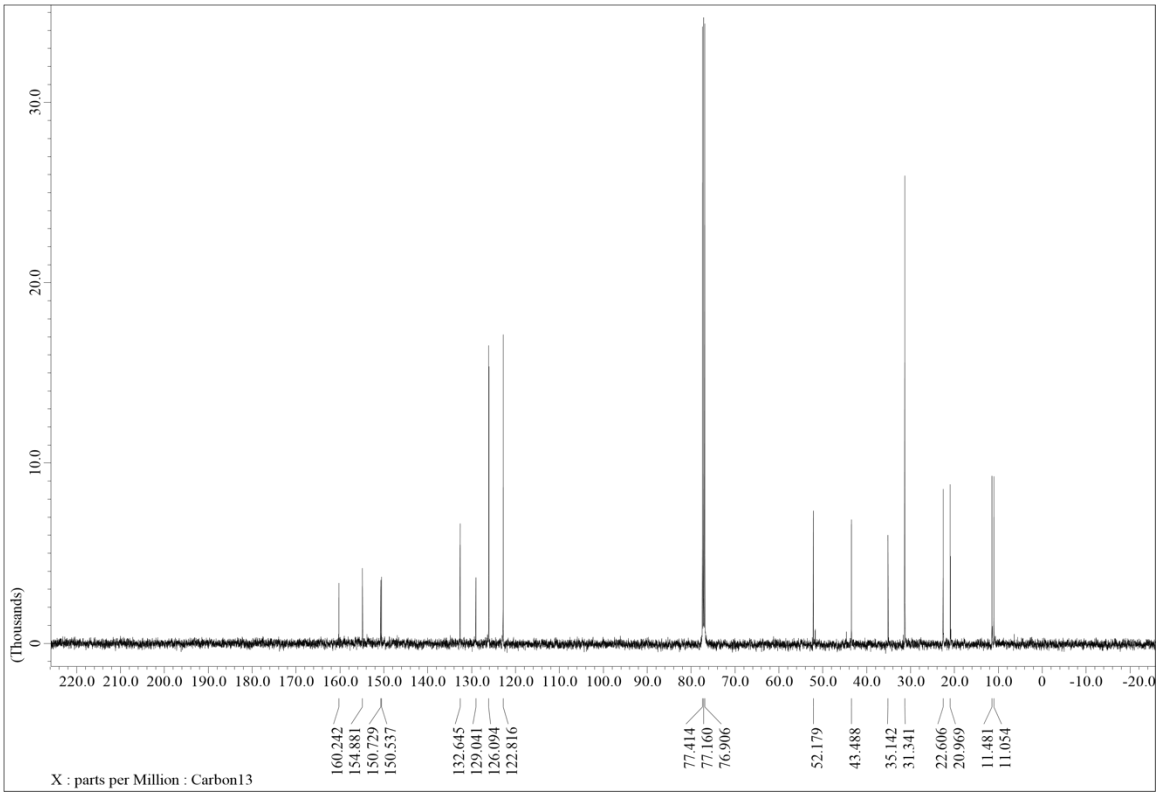

6-iodo-2,4-dioxo-1-propyl-3-hydropyrimidine. (9)

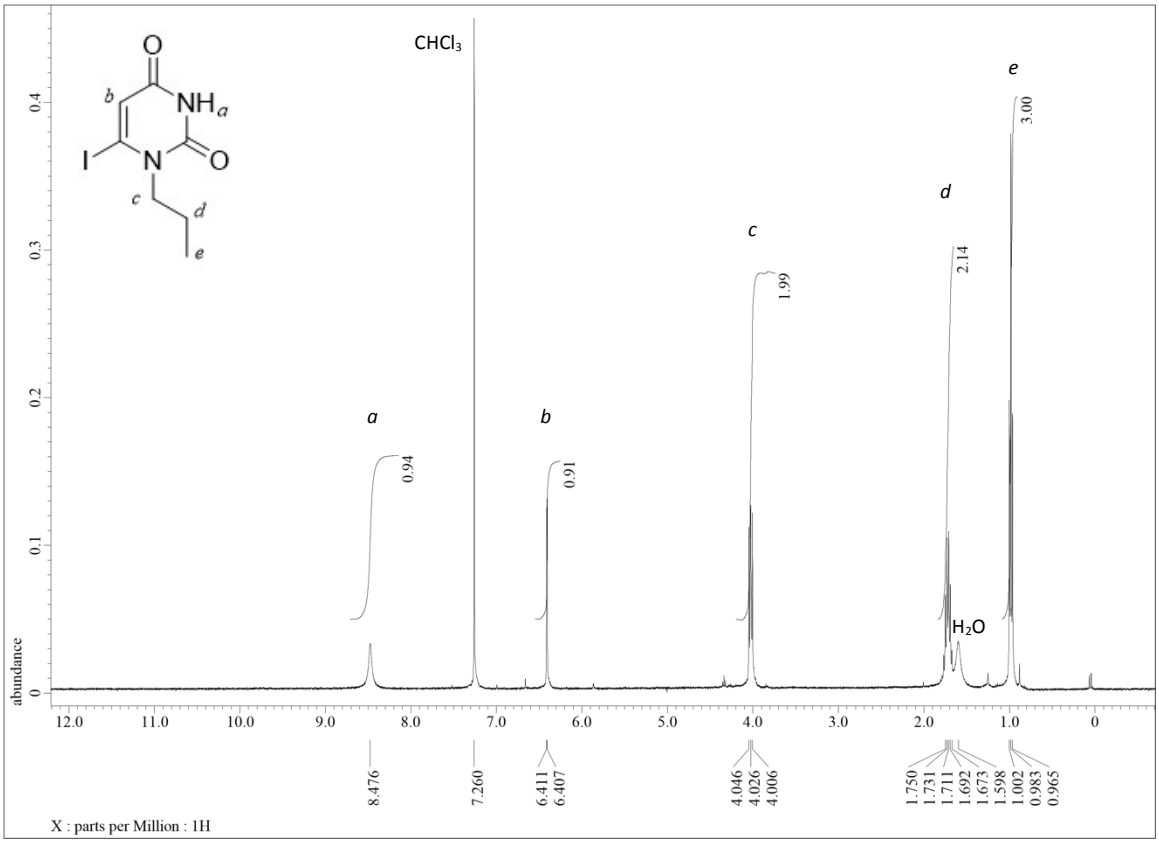

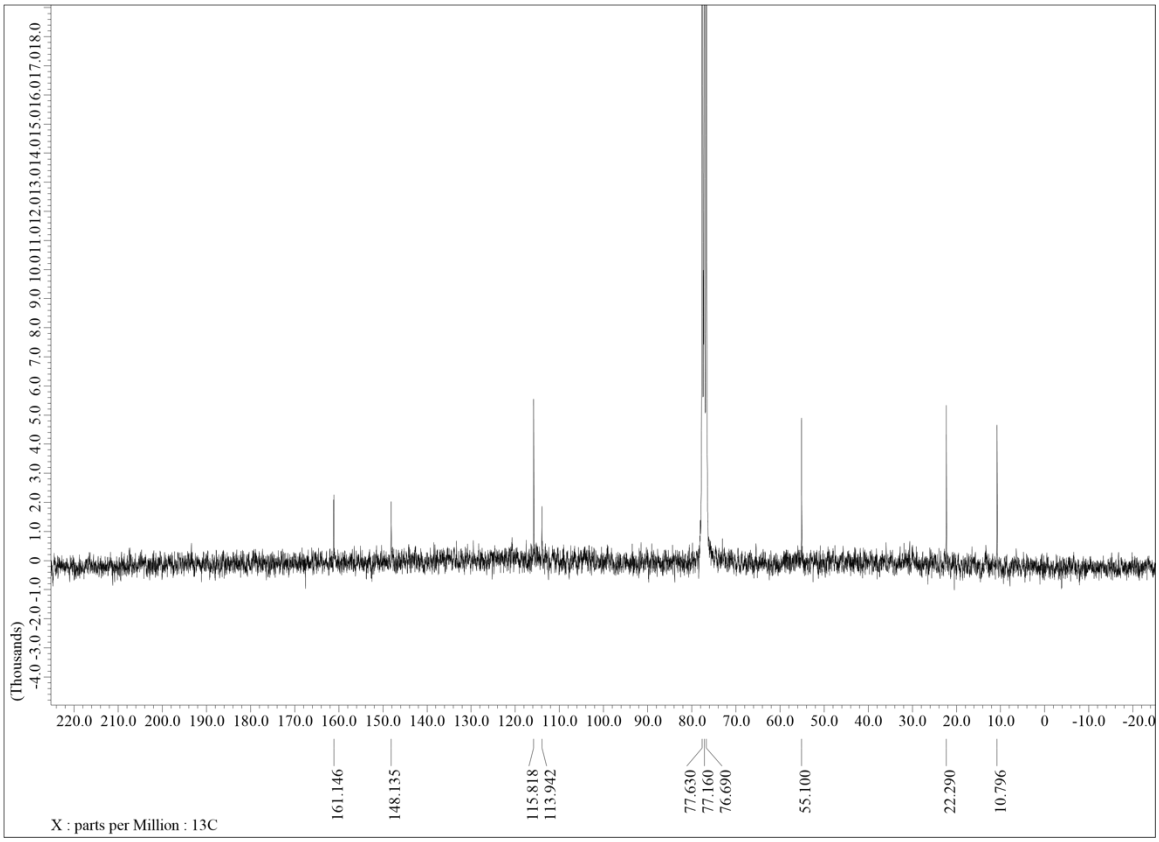

6-((4-(*tert*-butyl)phenyl)diazenyl)-2,4-dioxo-1-propyl-3-hydropyrimidine (10, 6AUP)

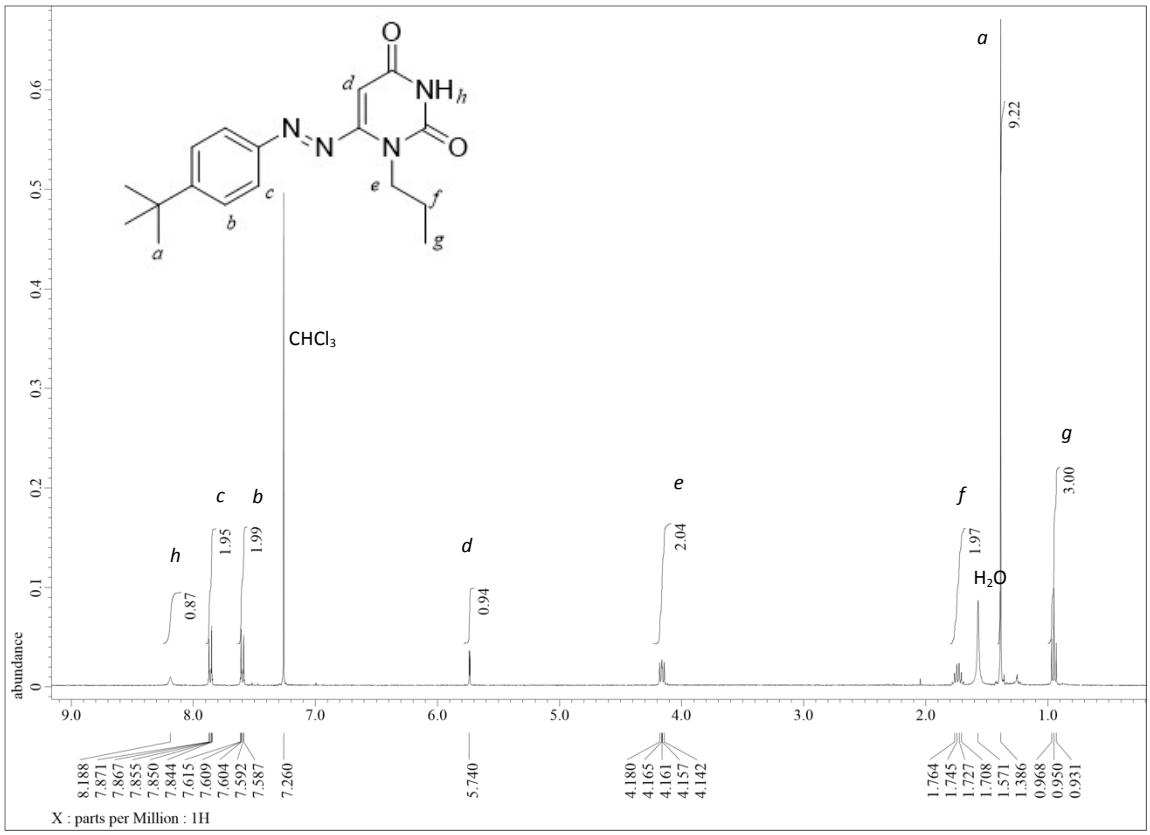

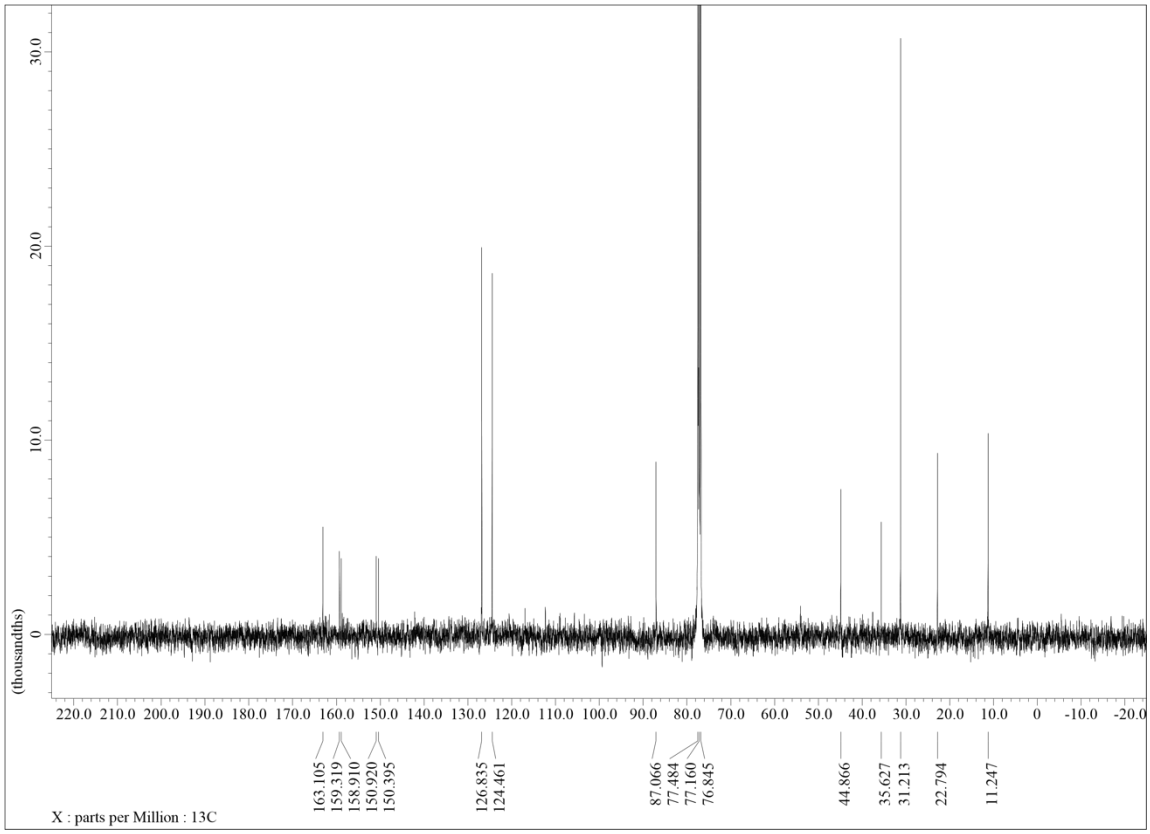

Mass analysis

Mass spectra of 5AUP (4)

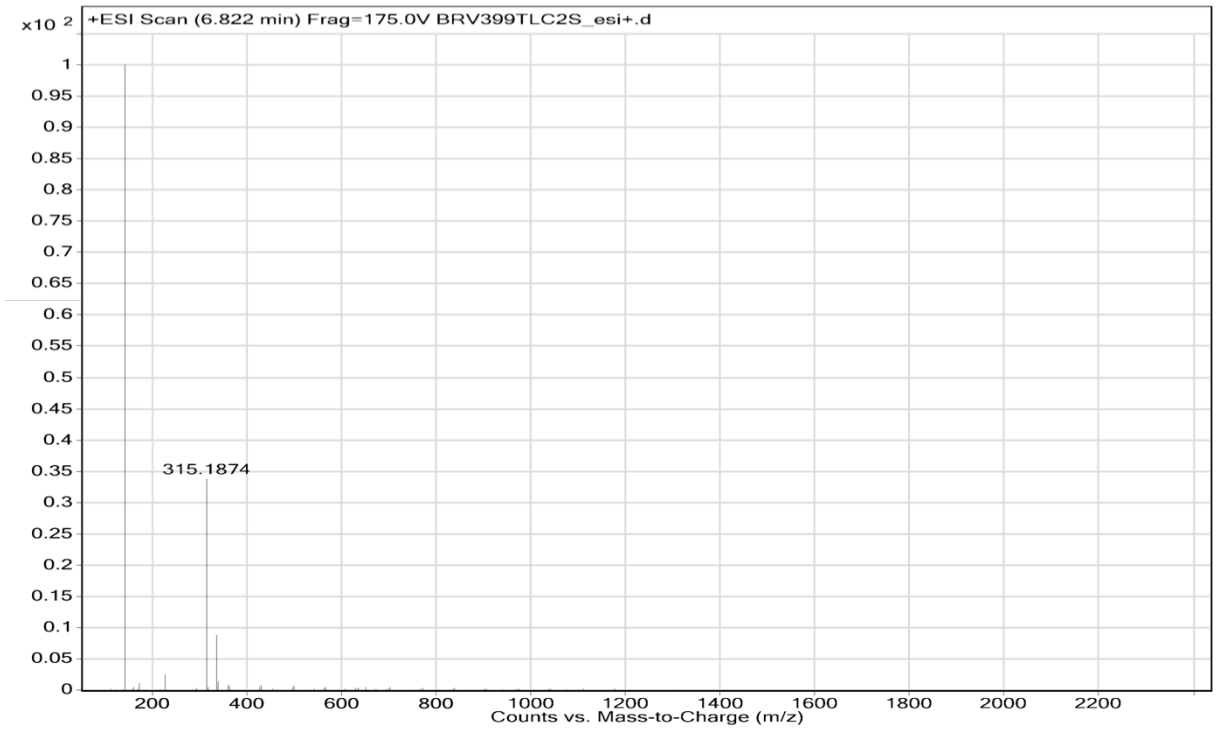

Mass spectra of 5AUPP (6)

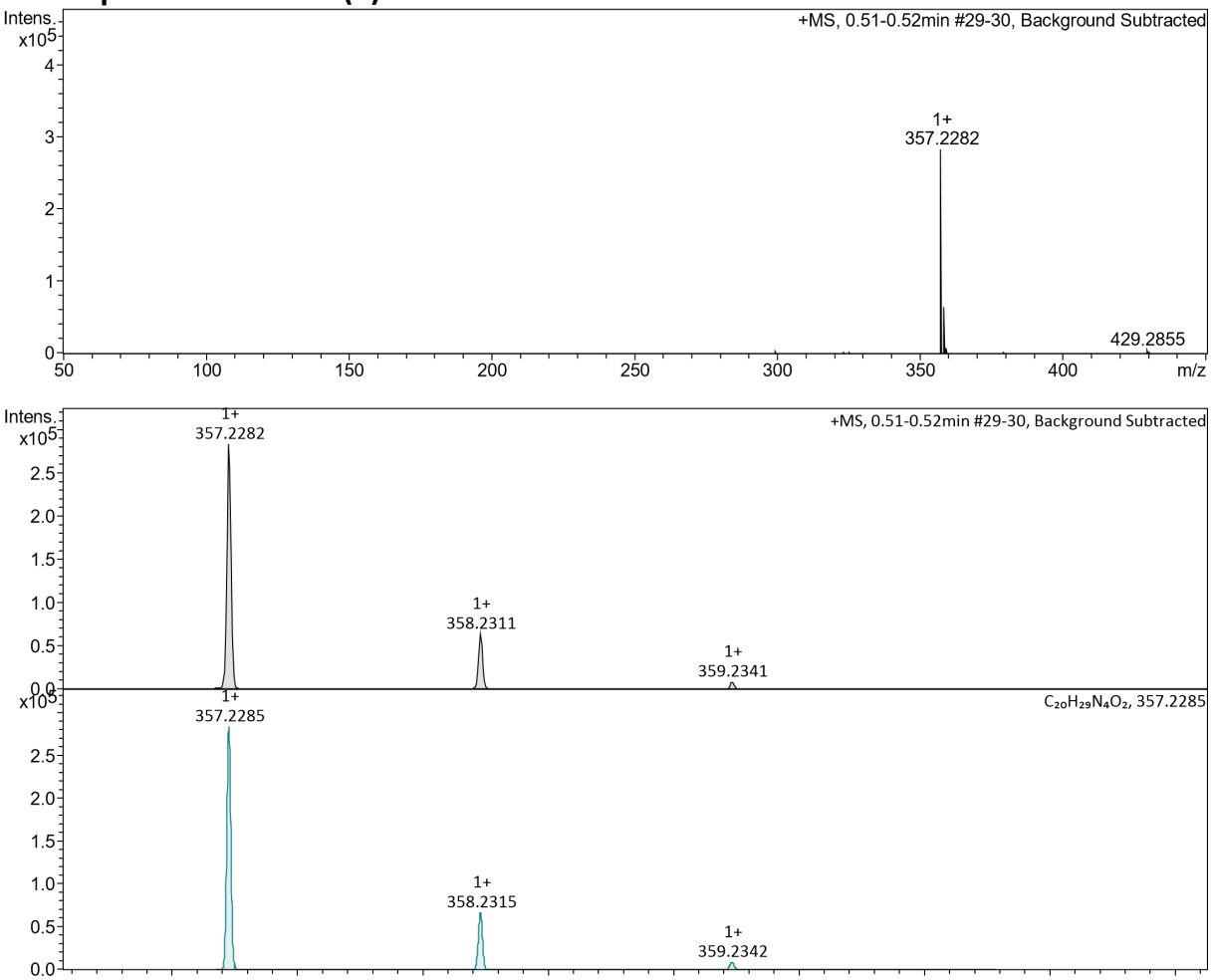

Mass spectra of 6AUP (10)

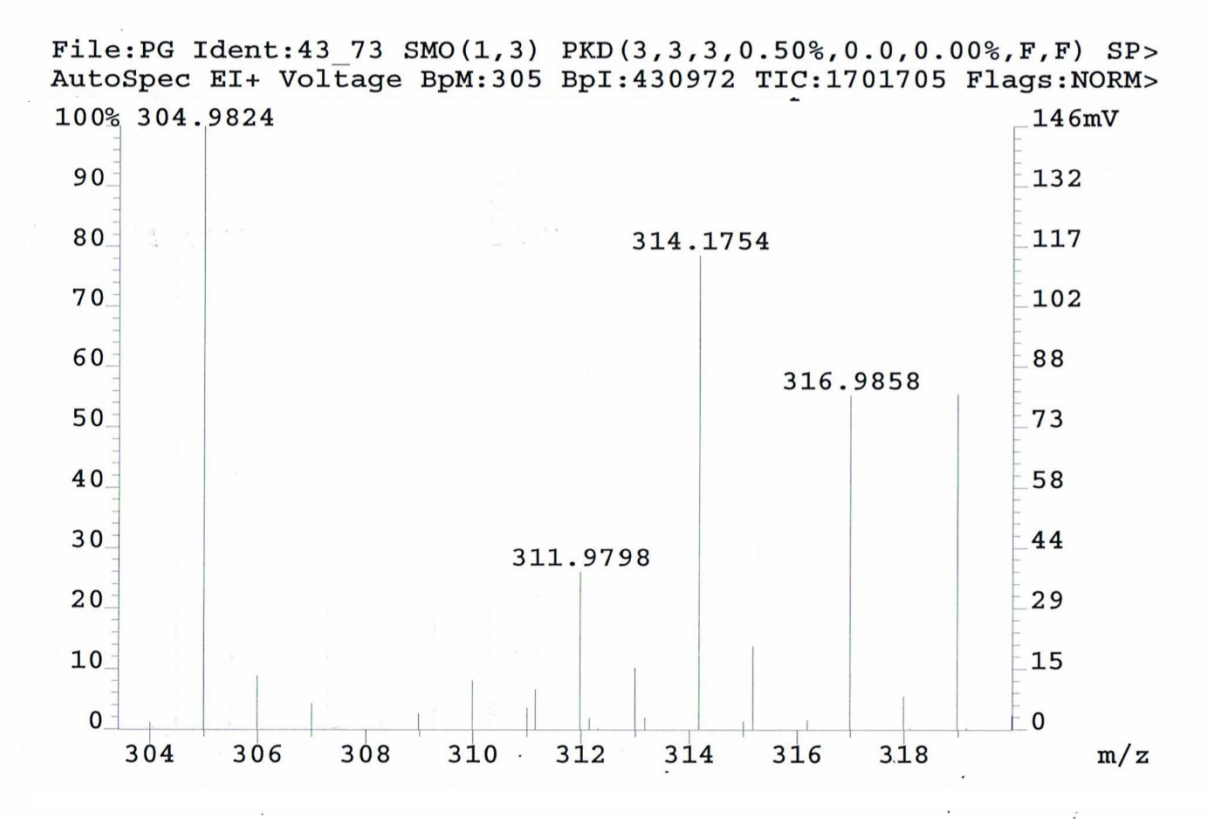

Crystal data and structure refinement

Table S1. Crystal data and structure refinement for 5AUP (CCDC 1435199)

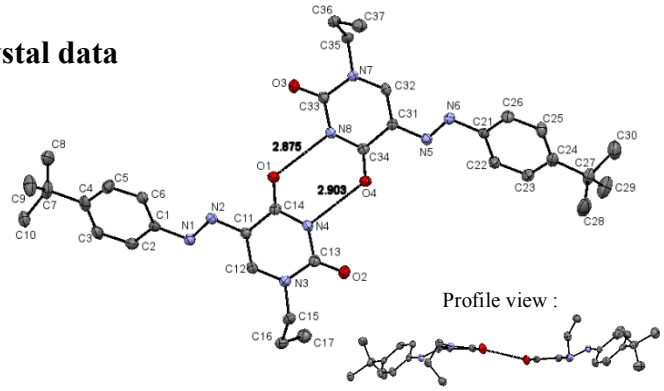

Crystal data		
Formula	$C_{17}H_{22}N_4O_2$	
Formula Weight	314.39	
Crystal system	Monoclinic	
Space group	$P2_1/n$	
Unit cell dimensions	a = 9.9256(5) Å	α = 90°
	b = 12.5657(7) Å	β = 95.471(5)°
	c = 25.9625(14) Å	γ = 90°
Volume	3223.3(3) $Å^3$	
Z	8	
Density (calculated)	1.296 g/cm^3	
Absorption coefficient	0.087 mm^{-1}	
F(000)	1344	
Crystal size	0.14 x 0.25 x 0.31 mm	
Data collection		
Temperature	150 K	
Wavelength	0.71073 Å	
Theta range for data collection	3.3 to 25.0°	
Index range	$-10 \le h \le 11$, $-14 \le k \le 14$, $-29 \le l \le 30$	
Reflections collected	14756	
Independent reflections	5355 [R(int) = 0.025]	
Observed data [$I > 2\sigma(I)$]	4509	
Refinement		
Data / restraints / parameters	5355 / 0 / 455	
R, wR2, S	0.0486, 0.1310, 1.04	
$w = 1/[(\sigma^2F_0^2)+(0.0567P)^2+2.1977P]$	where $P = (F_0^2+2F_c^2)/3$	
Largest diff. peak and hole	-0.31 and 0.72 $e.Å^{-3}$	

Table S2. Crystal data and structure refinement for 5AUP·DAP (CCDC1474613)

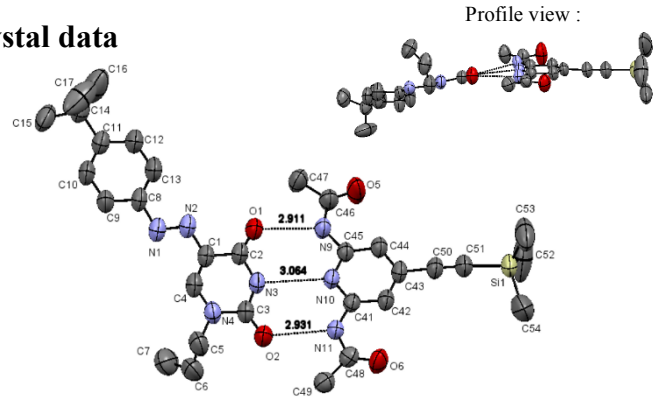

Crystal data	
Formula	$C_{31}H_{41}N_7O_4Si$
Formula Weight	603.80
Crystal system	Monoclinic
Space group	*P 21/c*
Unit cell dimensions	a = 19.5588(4) Å α = 90°
	b = 14.0407(3) Å β = 100.254(2)°
	c = 26.4137(7) Å γ = 90°
Volume	7137.9 (3) $Å^3$
Z	8
Density (calculated)	1.124 g/cm^3
Absorption coefficient	0.920 mm^{-1}
F(000)	2576
Crystal size	0.11 x 0.12 x 0.13 mm
Data collection	
Temperature	293 K
Wavelength	1.54184 Å
Theta range for data collection	3.4 to 66.6°
Index range	-23≤h≤16, -16≤k≤15, -30≤l≤31
Reflections collected	27063
Independent reflections	12394 [R(int) = 0.057]
Observed data [$I>2\sigma(I)$]	8015
Refinement	
Data / restraints / parameters	12394 / 41 / 847
R, wR2, S	0.0932, 0.3057, 1.10
$w = 1/[(\sigma^2F_0^2)+(0.1808P)^2+0.1103P]$	where $P = (F_0^2+2F_c^2)/3$
Largest diff. peak and hole	-0.53 and 0.71 $e.Å^{-3}$

Table S3. Crystal data and structure refinement for 6AUP (CCDC1435200)

Crystal data	
Formula	$C_{17}H_{22}N_4O_2$
Formula Weight	314.39
Crystal system	Triclinic
Space group	*P-1*
Unit cell dimensions	a = 8.2330(4) Å α = 75.055 (7)°
	b = 10.0136(9) Å β = 82.521(5)°
	c = 10.5735(7) Å γ = 87.889(6)°
Volume	853.04(10) $Å^3$
Z	2
Density (calculated)	1.250 g/cm^3
Absorption coefficient	0.681 mm^{-1}
F(000)	336.0
Crystal size	0.12 x 0.30 x 0.50 mm
Data collection	
Temperature	150 K
Wavelength	1.54184 Å
Theta range for data collection	5.4 to 66.6°
Index range	-8≤h≤9, -10≤k≤11, -12≤l≤12
Reflections collected	5541
Independent reflections	2865 [R(int) = 0.025]
Observed data [$I>2\sigma(I)$]	2639
Refinement	
Data / restraints / parameters	2865 / 0 / 216
R, wR2, S	0.0579, 0.1576, 1.11
$w = 1/[(\sigma^2F_0^2)+(0.0365P)^2+1.1541P]$	where $P = (F_0^2+2F_c^2)/3$
Largest diff. peak and hole	-0.17 and 0.21 $e.Å^{-3}$

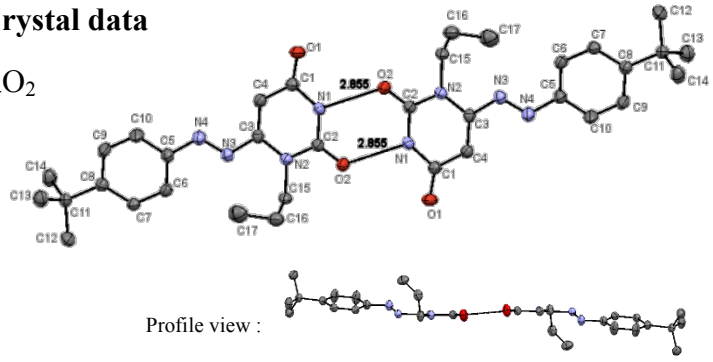

Table S4. Crystal data and structure refinement for 6AUP·DAP(CCDC1435201)

Crystal data	
Formula	$C_{31}H_{41}N_7O_4Si$
Formula Weight	603.80
Crystal system	Triclinic
Space group	*P-1*
Unit cell dimensions	a = 12.2322(7) Å α = 118.238(6)°
	b = 12.9303(8) Å β = 94.607(5)°
	c = 13.2865(7) Å γ = 107.892(5)°
Volume	1696.80(17) $Å^3$
Z	2
Density (calculated)	1.182 g/cm^3
Absorption coefficient	0.113 mm^{-1}
F(000)	644.0
Crystal size	0.18 x 0.26 x 0.48 mm
Data collection	
Temperature	293 K
Wavelength	0.71073 Å
Theta range for data collection	2.9 to 25.0°
Index range	-14≤h≤13, -15≤k≤15, -15≤l≤15
Reflections collected	13392
Independent reflections	5986 [R(int) = 0.026]
Observed data [I>2σ(I)]	4603
Refinement	
Data / restraints / parameters	5986 / 3 / 409
R, wR2, S	0.0770, 0.2225, 1.20
w = 1/[($\sigma^2F_0^2$)+(0.0926P)^2+0.9956P]	where P = (F_0^2+2F_c^2)/3
Largest diff. peak and hole	-0.66 and 0.90 e.$Å^{-3}$

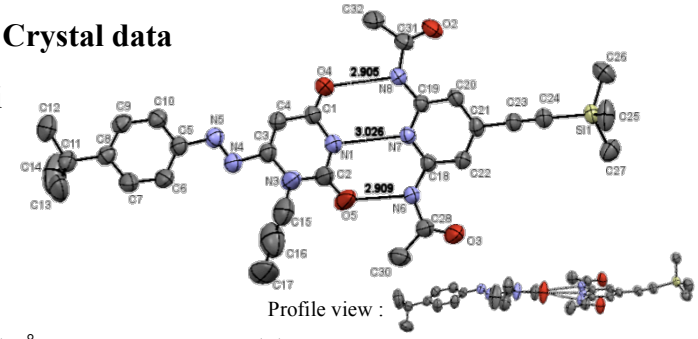

UV-Vis kinetic studies

Thermal *Z*→*E* isomerization of 5AUP.

The isomerization of *Z*-5AUP to its *E* diastereoisomer was monitored by UV-Vis analysis of a 5AUP solution (3.0 x 10^{-5} M in toluene) previously irradiated. The kinetic experiment was run by taking full scans of the irradiated solution. The extinction coefficient of the ***E*-5AUP** was determined in prior experiments and is: ε = 20727 M^{-1} cm^{-1}. The fitting of the experimental data, *i.e.* the absorbance change at λ_{max} over the time, (Fig. S1) was performed with Origin 8 considering a first order kinetic model and gives an observed rate constant k_{est}= (2.7 ± 0.01) x 10^{-5} s^{-1} and ΔA = 0.534.

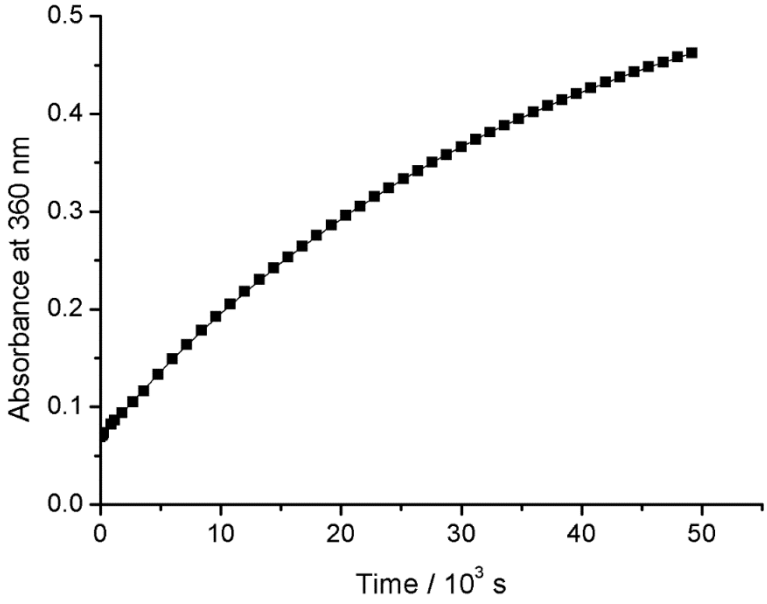

Figure S1. Fitting of the experimental data with a first order kinetic model.

Thermal *Z*→*E* isomerization of 5AUPP.

The isomerization of *Z*-5AUPP to its *E* diastereoisomer was monitored by UV-Vis analysis of a 5AUPP solution (5.2 x 10^{-5} M in toluene) previously irradiated. The kinetic experiments were run by recording the absorbance change at 364 nm, over a time span of 560 minutes. The extinction coefficient of the ***E*-5AUPP** was determined in prior experiments and is: ε = 12561 M^{-1} cm^{-1}. The fitting of the experimental data gives an observed rate constant k_{est}= (3.06 ± 0.03) x 10^{-5} s^{-1} and ΔA = 0.377.

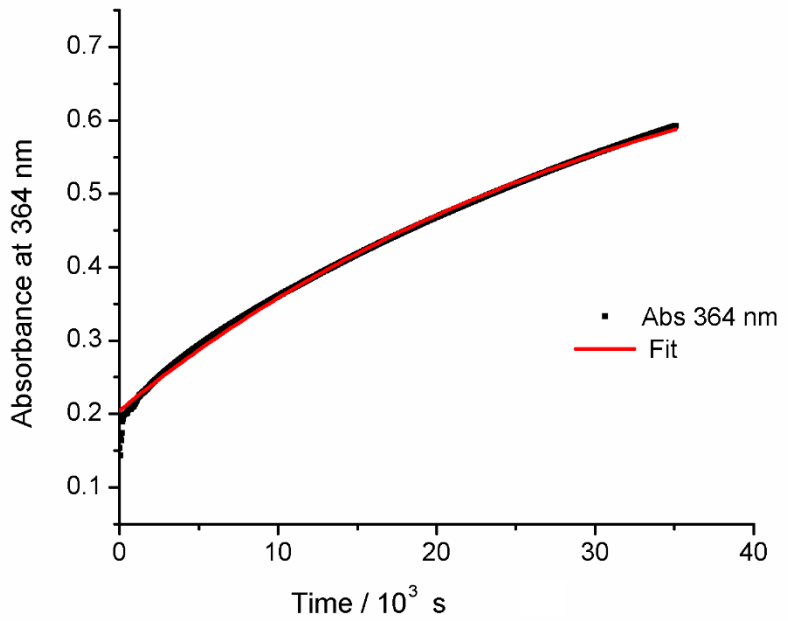

Figure S2. Fitting of the experimental data with a first order kinetic model.

^{1}H-NMR kinetic studies

Thermal *Z*→*E* isomerization of 5AUP.

The isomerization of *Z*-5AUP to its *E* diastereoisomer was studied also by ^{1}H NMR analysis of a 5AUP solution (3.0 mM in toluene-d_8) previously irradiated, by monitoring the initial rate of formation of the *E* isomer. The analysis of the experimental data was performed according to the initial rate method, the isomerization rate is given by the slope of the straight lines reported in Figure S3; the initial concentration of *Z*-**5AUP** ($[Z]_0$) is instead given by the intercept of the straight line describing the consumption of *Z*-**5AUP**. The composition of the reaction mixture as a function of time is reported in Table S5 and Fig. S3.

Table S5. Experimental data for the *Z* to *E* isomerization of *Z*-**5AUP** monitored by ^{1}H NMR experiments.

Time (s)	integral N-CH_2 *E*	integral N-CH_2 *Z*	% *Z*	% *E*	[*E*] (mM)	[*Z*] (mM)
600	0.01926	0.26	93.1	6.9	0.206904	2.793
780	0.01949	0.26	93.0	7.0	0.209202	2.791
1200	0.02233	0.26	92.1	7.9	0.237276	2.763
1440	0.02533	0.26	91.1	8.9	0.266323	2.734
1620	0.02655	0.26	90.7	9.3	0.277962	2.722
1800	0.02589	0.26	90.9	9.1	0.271678	2.728
1980	0.02954	0.26	89.8	10.2	0.306072	2.694
2280	0.0298	0.25	89.3	10.7	0.319514	2.68

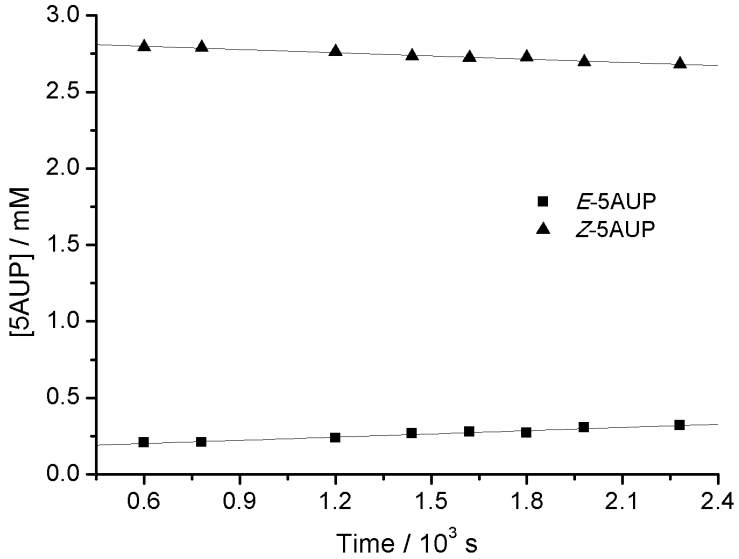

Figure S3. Linear fitting of the experimental data according to the initial rate method.

The results of the fitting are reported in Table S6 for both the formation of *E*-**5AUP** and the consumption of *Z*-**5AUP**.

Table S6. Fitting data for the *Z*-**5AUP** to *E*-**5AUP** isomerization.

	slope (M^{-1} s^{-1})	Standard Error (M^{-1} s^{-1})	Intercept (M)	Standard Error (M)
Z	-7.03 x 10^{-8}	5.38 x 10^{-9}	0.00284	8.39 x 10^{-6}
E	7.03 x 10^{-8}	5.38 x 10^{-9}	1.59 x 10^{-4}	8.39 x 10^{-6}
k_{obs} (s^{-1})	δk (s^{-1})			
2.48 x 10^{-5}	1.97 x 10^{-6}			

Considering that at the beginning of the reaction, the mixture contains 2.84 mM *Z*-**5AUP**, the observed rate constant for the *Z*-*E* isomerization is: k_{est} = (2.48 ± 0.20) x 10^{-5} s^{-1}. The calculation of the uncertainty was performed by using the uncertainty propagation method.

Thermal *Z*→*E* isomerization of 5AUP in the presence of DAP

The isomerization of *Z*-5AUP to its *E* diastereoisomer in the presence of increasing amounts of DAP was monitored by ^{1}H-NMR analysis of toluene-d_8 solutions previously irradiated. The conditions explored were the following: ***Z*-5AUP:DAP=8:2** ([5AUP] = 2.9 mM and [DAP] = 0.73 mM) and ***Z*-5AUP:DAP =1:1** ([5AUP] = 2.5 mM and [DAP] = 2.5 mM), where the **nominal [5AUP]** are those of the prepared solutions **before irradiation**, the reactions were monitored for 140 and 45 minutes respectively.

Conditions: ***Z*-5AUP:DAP =8:2** ([5AUP] = 2.9 mM and [DAP] = 0.73 mM).

The experimental data are reported in Table S7, the analysis was restricted to the first instants of the reaction according to the initial rate method and represented graphically in Figure S4 while the results of the fitting are reported in Table S8.

Table S7. Experimental NMR data for the isomerization of *Z*-5AUP to *E*-5AUP in the presence of DAP, ***Z*-5AUP: DAP =8:2**

Time (s)	integral N-CH_2 *Z*	integral N-CH_2 *E*	% *E*	% *Z*	[*E*] (mM)	[*Z*] (mM)
600	8.59	0.89	9.4	90.6	0.272257	2.628
900	8.49	0.97	10.3	89.7	0.297357	2.603
1500	8.08	1.1	12.0	88.0	0.347495	2.553
1860	7.96	1.12	12.3	87.7	0.357709	2.542
2340	7.78	1.32	14.5	85.5	0.420659	2.479
2940	6.75	1.21	15.2	84.8	0.440829	2.459
4560	6.37	1.59	20.0	80.0	0.579271	2.321
5340	6.03	1.75	22.5	77.5	0.652314	2.248
6540	5.55	1.72	23.7	76.3	0.686107	2.214
8340	5.39	1.98	26.9	73.1	0.779104	2.121
12360	4.55	2.46	35.1	64.9	1.017689	1.882
13140	4.58	2.51	35.4	64.6	1.026657	1.873

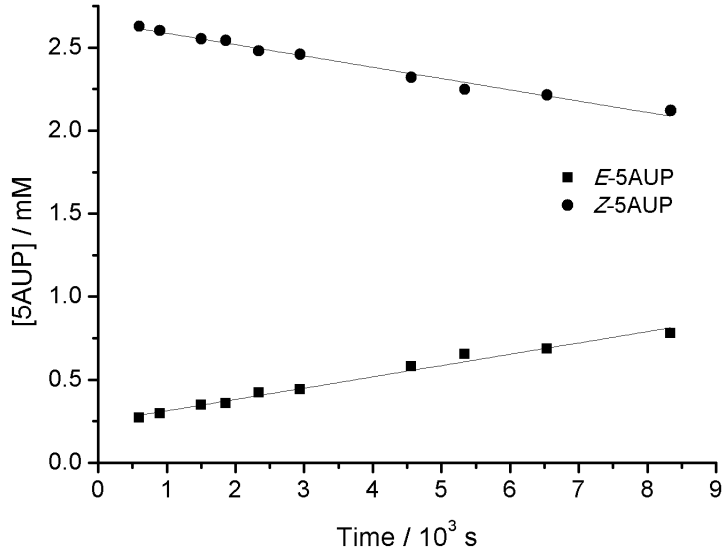

Figure S4. Linear fitting of the experimental data according to the initial rate method.

Table S8. Fitting data for the *Z*-5AUP to *E*-5AUP isomerization in the following conditions: (***Z*-5AUP: DAP =8:2**).

	slope (M^{-1} s^{-1})	Standard Error (M^{-1} s^{-1})	Intercept (M)	Standard Error (M)
Z	-6.81×10^{-8}	3.00×10^{-9}	0.00265	1.28×10^{-5}
E	6.81×10^{-8}	3.00×10^{-9}	2.46×10^{-4}	1.28×10^{-5}
k_{obs} (s^{-1})	δk (s^{-1})			
2.57×10^{-5}	1.26×10^{-6}			

Considering that at the beginning of the reaction the concentration of *Z*-**5AUP** is 2.65 mM (see intercept in Table S8), and using the slopes reported in Table S8, the observed rate constant for the *Z* to *E* isomerization results: $k_{obs} = (2.57 \pm 0.13) \times 10^{-5}$ s^{-1}, the uncertainty was calculated as in the preceding cases.

Conditions: ***Z*-5AUP:DAP =1:1** ([5AUP] = 2.5 mM and [DAP] = 2.5 mM).

In this case the N-CH_2 protons of the *Z* and *E* form were not distinguishable, therefore all values reported were calculated taking in consideration the integral of the NH proton.

The experimental data are reported in Table S9, the analysis was restricted to the first instants of the reaction as before and represented graphically in Figure S5 while the results of the fitting are reported in Table S10.

Table S9. Experimental NMR data for the isomerization of *Z*-5AUP to *E*-5AUP in the presence of DAP, ***Z*-5AUP:DAP =1:1**.

Time (s)	integral N-H *Z*	integral N-H *E*	% *E*	% *Z*	[*E*] (mM)	[*Z*] (mM)
420	0.96	0.18	15.8	84.2	0.394737	2.105263
840	0.95	0.25	20.8	79.2	0.520833	1.979167
960	0.9	0.26	22.4	77.6	0.560345	1.939655
1260	0.87	0.27	23.7	76.3	0.592105	1.907895
1380	0.85	0.31	26.7	73.3	0.668103	1.831897
1560	0.8	0.33	29.2	70.8	0.730088	1.769912
1740	0.77	0.34	30.6	69.4	0.765766	1.734234
2220	0.74	0.35	32.1	67.9	0.802752	1.697248
2640	0.69	0.42	37.8	62.2	0.945946	1.554054

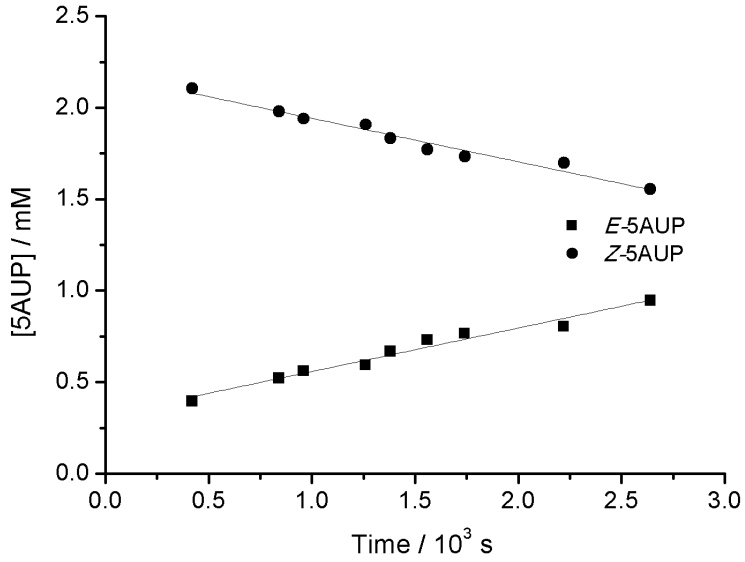

Figure S5. Linear fitting of the experimental data according to the initial rate method.

Table S10. Fitting data for the *Z*-5AUP to *E*-5AUP isomerization in the following conditions: (***Z*-5AUP:DAP = 1:1**).

	slope (M^{-1} s^{-1})	Standard Error (M^{-1} s^{-1})	Intercept (M)	Standard Error (M)
Z	-2.38×10^{-7}	1.56×10^{-8}	0.00218	2.48×10^{-5}
E	2.38×10^{-7}	1.56×10^{-8}	3.21×10^{-4}	2.48×10^{-5}
k_{obs} (s^{-1})	δk (s^{-1})			
1.09×10^{-4}	8.41×10^{-6}			

Considering that at the beginning of the reaction, the actual concentration of *Z*-**5AUP** is 2.18 mM and using the slopes reported in Table S10, the observed rate constant results k_{obs} = (1.09 ± 0.08) x 10^{-4} s^{-1}.

The experimental results for the thermal isomerization in the absence of **DAP**, and in presence of variable DAP concentration (*Z*-**5AUP**: **DAP** =1:1 and *Z*-**5AUP**:**DAP** =8:2), are plotted together in the graph of Figure S6.

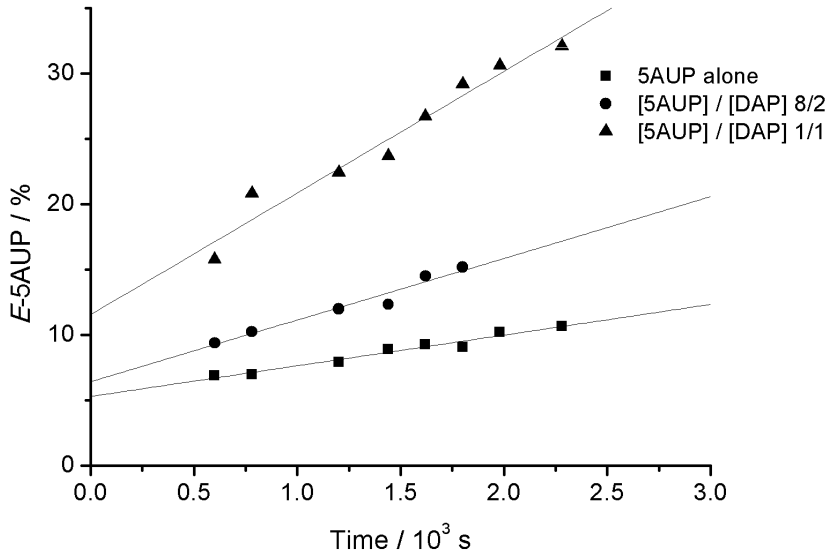

Figure S6. Rates of formation of *E*-**5AUP** in the absence of **DAP**, (squares), in the presence of 0.73 mM **DAP** (circles) corresponding to a *Z*-**5AUP**: **DAP** =8:2 ratio, and 2.5 mM **DAP** corresponding to *Z*-**5AUP**:**DAP** =1:1 (triangles).

From inspection of Figure S6 it is clear how the residual amount of *E*-**5AUP** present since the beginning of the reaction (see intercept of the fitting lines), increases at increasing concentrations of **DAP**. The isomerization rate also increase with the increasing of the concentration of **DAP**; the values of the rate constants for the three conditions are summarized in Table S11.

Table S11. Rate constants for the *Z*-5AUP to *E*-5AUP isomerization in the presence of increasing concentrations of DAP.

	[5AUP] (M)	[DAP] (M)	k_{obs} (s^{-1})	δk_{obs} (s^{-1})
no **DAP**	3.0×10^{-3}	-	2.48×10^{-5}	1.97×10^{-6}
5AUP: **DAP** = 8:2	2.9×10^{-3}	0.73×10^{-3}	2.57×10^{-5}	1.26×10^{-6}
5AUP: **DAP** = 1:1	2.5×10^{-3}	2.5×10^{-3}	1.09×10^{-4}	0.08×10^{-4}

Thermal *Z*→*E* isomerization of 5AUP in the presence of DAP excess

The isomerization of *Z*-5AUP was monitored by ^{1}H NMR also in the presence of DAP excess, the experiments were run in the conditions summarized in Table S12. At variance with the previous case, the concentration of DAP was maintained constant at about 10 mM while 5AUP was used at the nominal concentrations (before irradiation) [**5AUP**] equal to 1.0 mM, 2.2 mM and 3.2 mM, see entries Ex1, Ex2 and Ex3 in Table S12 respectively.

Table S12. Conditions for the *Z*-5AUP to *E*-5AUP isomerization experiments at varying concentrations of *Z*-5AUP and in the presence of a **DAP excess**.

	[5AUP] (mM)	$[DAP]_0$ (mM)
Ex1	1.00	9.40
Ex2	2.2	9.6
Ex3	3.2	10.2

The concentration of ***E*-5AUP** measured in the first 50 minutes of reaction are reported in Table S13 and displayed graphically in Figure S7. These data were used for assessing the initial reaction rate in the different conditions and for the calculation of the pertinent rate constants.

Table S13. Experimental data for the *Z*-5AUP to *E*-5AUP isomerization experiments at varying concentrations of *Z*-5AUP in the presence of a **DAP excess**.

Ex1 [5AUP] = 1.0 mM		***Ex2*** [5AUP] = 2.2 mM		***Ex3*** [5AUP] = 3.2 mM	
Time (s)	[*E*-5AUP] (mM)	Time (s)	[*E*-5AUP] (mM)	Time (s)	[*E*-5AUP] (mM)
660	0.277	780	0.628571	600	1.434978
1080	0.308	1380	0.750853	900	1.624365
1680	0.342	1980	0.827068	1500	1.797753
2340	0.392	2580	0.90535	2100	1.849711
2880	0.411	3180	0.940171	2700	2.038217

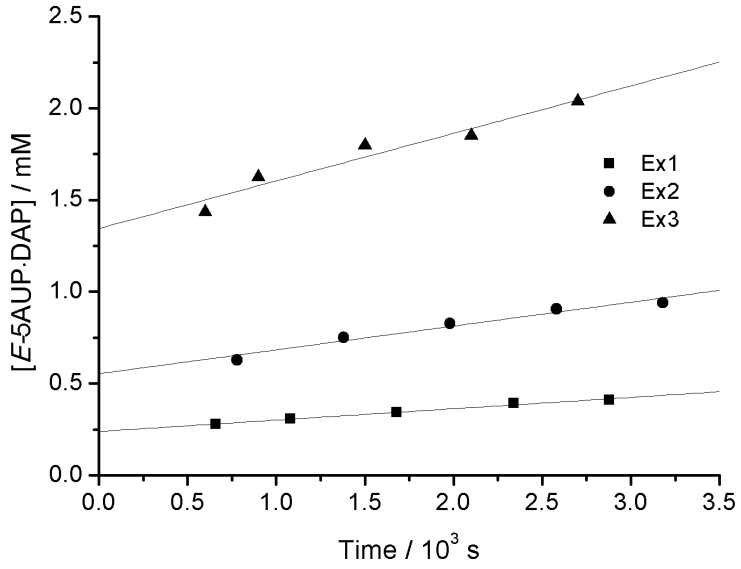

Figure S7. Linear fitting of the experimental data according to the initial rate method.

The observed rate constants are reported in Table S14, together with the actual initial concentration of *Z*-5AUP estimated from the intercept of the straight line describing the consumption of *Z*-5AUP. The uncertainties of the rate constants were calculated according to the uncertainty propagation method.

Table S14. Observed rate constants for the *Z*-5AUP to *E*-5AUP isomerization experiments at varying initial concentrations of *Z*-5AUP in the presence of a **DAP excess**.

	[*Z*-5AUP] (M)	[DAP] (M)	k_{obs} (s^{-1})	δk_{obs} (s^{-1})
Ex1	7.6×10^{-4}	9.4×10^{-3}	8.1×10^{-5}	1×10^{-6}
Ex2	1.6×10^{-3}	9.6×10^{-3}	7.9×10^{-5}	1×10^{-5}
Ex3	1.8×10^{-3}	10.2×10^{-3}	1.4×10^{-4}	3×10^{-5}

The observed rate constants determined in the three cases are the same within the experimental uncertainty with an average $k_{iso} \approx (1.0 \pm 0.3) \times 10^{-4}$ s^{-1}. By comparing this value with the rate constant for the thermal isomerization of *Z*-5AUP in the absence of DAP obtained by NMR, $k_{est} = 2.5 \times 10^{-5}$ s^{-1}, the acceleration of the *Z*-*E* isomerization within the complex can be calculated as $k_{iso}/ k_{est} = 4$.

^{1}H-NMR complexation studies

Determination of complex stoichiometry.

The 1:1 binding stoichiometry of the *E*-5AUP·DAP and Upr·DAP complexes was confirmed by Job's plot analysis.

Table S15. Experimental data for the ***E*-5AUP·DAP** Job's plot, obtained with non irradiated stock solutions of 5AUP (3.0 mM in toluene-d_8) and of DAP (3.0 mM in toluene-d_8).

V *E*-5AUP (mL)	$[E\text{-5AUP}]_0$ (mM)	V DAP (mL)	$[DAP]_0$ (mM)	$x_{E\text{-5AUP}}$	δ (ppm)	[*E*-5AUP·DAP] (mM)
0.05	0.30	0.45	2.7	0.10	11.776	0.30217
0.10	0.60	0.40	2.4	0.20	11.649	0.58537
0.15	0.91	0.35	2.1	0.30	11.469	0.8377
0.25	1.5	0.25	1.5	0.50	10.636	1.08495
0.30	1.8	0.20	1.2	0.60	9.968	1.00246
0.35	2.1	0.15	0.91	0.71	9.239	0.78823
0.40	2.4	0.10	0.61	0.81	8.629	0.5362
0.45	2.7	0.05	0.30	0.91	8.127	0.26563
0.50	3.0	0	0	1.0	7.732	0

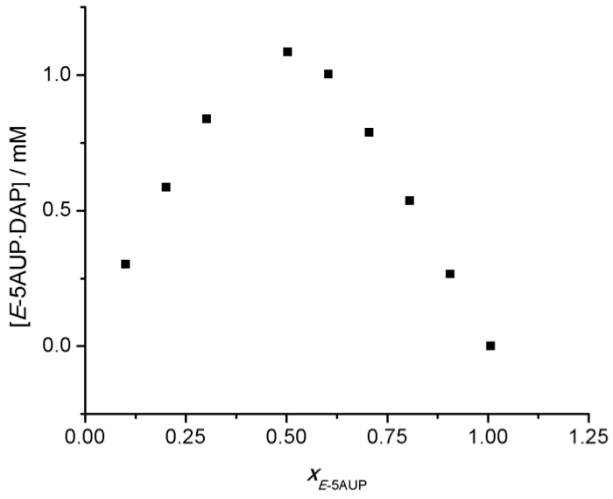

Figure S8. Job's plot for the ***E*-5AUP·DAP** complex.

Table S16. Experimental data for the **Upr·DAP** Job's plot, obtained with stock solutions of Upr (3.0 mM in toluene-d_8) and of DAP (3.0 mM in toluene-d_8).

V Upr (mL)	$[Upr]_0$ (mM)	V DAP (mL)	$[DAP]_0$ (mM)	x_{Upr}	δ (ppm)	[Upr·DAP] (mM)
0.05	0.30	0.45	2.7	0.10	11.830	0.30
0.10	0.61	0.40	2.4	0.20	11.733	0.59
0.15	0.91	0.35	2.1	0.30	11.599	0.86
0.25	1.5	0.25	1.5	0.51	10.749	1.1
0.30	1.8	0.20	1.2	0.61	9.799	0.90
0.35	2.1	0.15	0.91	0.71	9.171	0.71
0.40	2.4	0.10	0.61	0.81	8.590	0.46
0.45	2.7	0.05	0.30	0.91	8.153	0.21
0.50	3.0	0	0	1.0	7.849	0

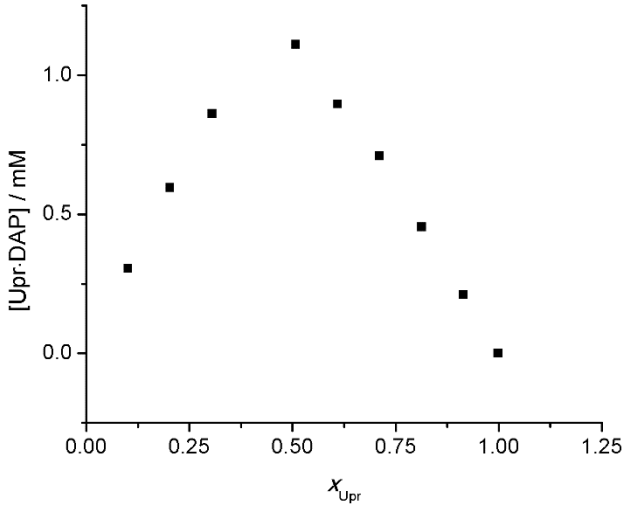

Figure S9. Job's plot for the **Upr·DAP** complex.

Dimerization of *E*-5AUP.

The dimerization equilibrium of *E*-5AUP was investigated in toluene-d_8 at 25 °C with a dilution experiment in which the concentration of 5AUP was varied in the interval 0.00076 – 0.0075 M. The dependence of the chemical shift of the imide proton from the concentration of 5AUP is shown in Figure S10 together with the fitting curves obtained with Dynafit.

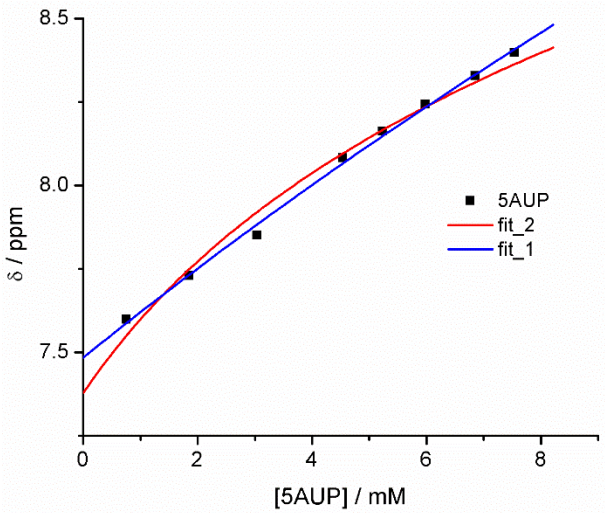

Figure S10. Fitting of the dimerization data with all the parameters free to be optimized (fit_1) and fixing the δ of the dimer at 12 ppm (fit_2).

The fitting of the dimerization experiment is problematic because in the range of concentration explored the dependence of the chemical shift from the concentration of 5-AUP is almost linear. Fitting of the data optimizing all the three parameters of the dimerization equation (K_{dim}, δ_0, and δ_{max} which are the dimerization constant and the chemical shift of the imide proton of monomer and dimer, respectively) gives an apparently good fit with a low value of dimerization constant (K_{dim} = 6 ± 5.9 M^{-1}) but an unacceptable estimation of the chemical shit of the dimer (δ_{max} = 30 ± 20 ppm) and a very large uncertainty on both parameters (blue curve in Figure S10). More reliable results are obtained by keeping fixed the δ_{max} at a value of 12 ppm, which is about the maximum chemical shift value of the imide proton in the complex with DAP, and optimizing the remaining two parameters (red curve in Figure S10). With this assumption the fitting gives K_{dim} = 55 ± 5 M^{-1} and δ_0 = 7.38 ± 0.5 ppm. These data are clearly affected by some uncertainty and the K_{dim} is probably overestimated, but due to the linear trend of the experimental points and to the fitting results we can safely assume that in any case the K_{dim} is lower than 100 M^{-1}. Based on this low value we consider that the dimerization equilibrium does not influence the formation of the complex.

Dimerization of Upr.

The dimerization equilibrium of Upr was investigated in toluene-d_8 at 25 °C with a dilution experiment in which the concentration of Upr was varied in the interval 0.0005 – 0.005 M. The problems for the fitting are the same as above (Fig. S11). Forcing the final chemical shift of the imide proton in the dimer (δ_{max}) to 12 ppm a K_{dim} = 65 M^{-1} (sd = 5.8) and a δ_0 = 7.25 ppm (sd = 0.043) are obtained.

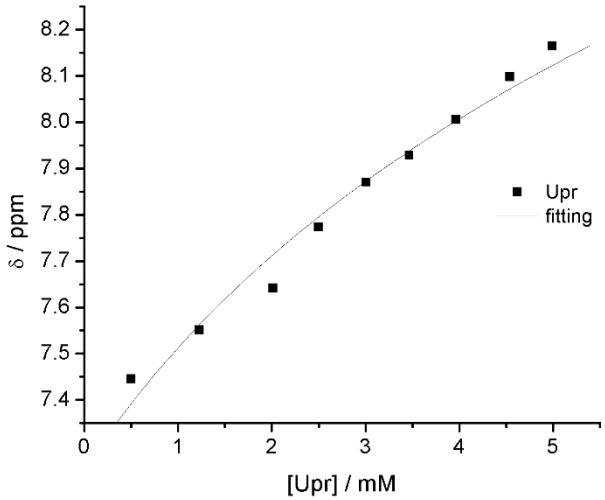

Figure S11. Fitting of the dilution experiment fixing the δ of the dimer at 12 ppm.

Titration of *E*-5AUP.

Three independent titration experiments have been made in toluene-d_8 at 25 °C, without sample irradiation. (Table S17)

Table S17. Conditions employed in three different titration experiments of *E*-5AUP complexation upon DAP addition.

	[5AUP] (mM)	[DAP] range (mM)
E1	3.022	0 - 8.8
E2	3.002	0 - 8.4
E3	2.9	0 – 8.5

The first titration (E3) shows some random broad peaks. This problem is resolved in the following titrations (E1 and E2) simply by waiting few minutes before to record the spectra after the addition of the guest. This is probably due to some aggregation of the guest.

The chemical shift data of the N-H imide proton of 5AUP were fitted against the guest concentration with Dynafit software packages using a 1:1 binding model. The solutions were prepared at the nominal concentration reported in Table S17 and during the fitting the concentration was optimized as a parameter. In this way, better fitting were obtained. The difference between the nominal and the calculated concentration of 5AUP vary in the three experiments and in any case is below 14%. The fitting of the three titrations are reported in Figure S12.

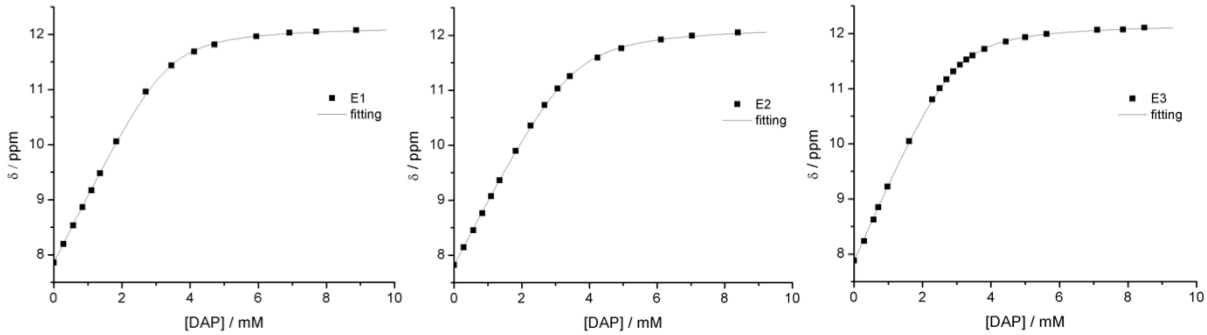

Figure S12. Fitting of the experimental data obtained from the titrations of *E*-5AUP with DAP.

The results of the fittings are reported in Table S18.

Table S18. Fitting data for the three titration experiments.

	K (M^{-1})	sd	δ_{max}	sd	[5AUP] (M)	sd	K_{mean} (M)	Sd
E1	7540	840	12.165	0.024	0.003363	3.60E-05		
E2	5630	540	12.184	0.026	0.003528	3.20E-05		
E3	6960	480	12.2	0.016	0.002955	2.70E-05	**6710**	**800**

The mean value of the association constant is $K_E = 6710 \pm 800\ M^{-1}$.

Titration of *Z*-5AUP.

Three independent titration experiments have been made in toluene-d_8 at 25 °C, in the conditions reported in Table S19, where the **nominal [5AUP]** are those of the prepared solutions **before irradiation**.

Table S19. Conditions employed in three different titration experiments of *Z*-**5AUP** complexation upon DAP addition.

	[5AUP] (M)	[DAP] range (M)
Z1	0.00305	0 – 0.0084
Z2	0.00378	0 – 0.0069
Z3	0.00407	0 – 0.00696

The analysis of these titrations is more complex because during the experiment *Z*-5AUP isomerizes to *E*-5AUP which competes for DAP. However, from the integration of the NMR peaks the concentration of *Z*- and *E*-5AUP at any moment of the titration experiment are known. The titration data were therefore fitted with Dynafit, that accepts more than one independent variable, using the following model:

Z + DAP <==> Z·DAP : Kc association

E + DAP <==> E·DAP : Kt association

The model takes in account the two equilibria *Z*/*E* + DAP and uses as independent variables the concentration of DAP, and the concentrations of *Z* and *E*-5AUP obtained from the

integration of the NMR spectra. The model fits the chemical shift data of the imide proton of the *Z*-5AUP and has 4 parameters: the two association constants and the initial and final chemical shift of the imide proton in the *Z*-5AUP·DAP complex. The K_E is kept constant at the value of 6710 M^{-1}, determined in the titration of *E*-5AUP with DAP (see above), as well as the initial value of the chemical shift at the experimental observed one. Therefore, the output is the K_Z and the value of the chemical shift in the *Z*-5AUP·DAP complex. The fittings are reported in Figure S13 and the data in Table S20.

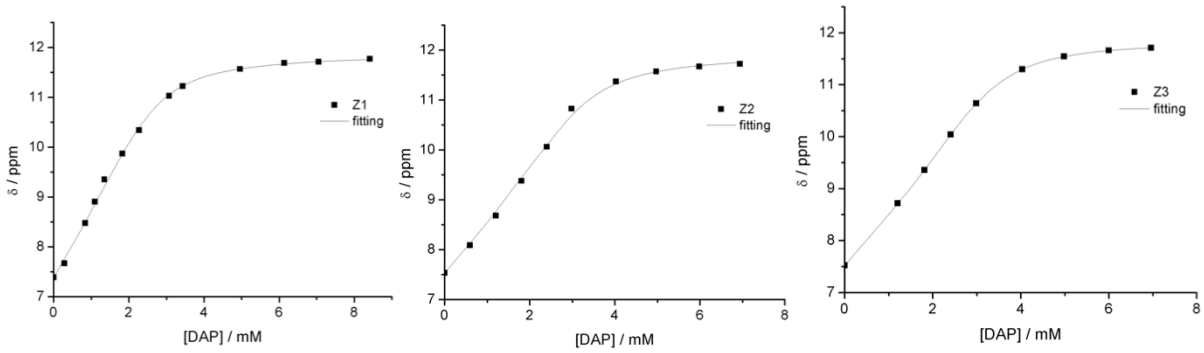

Figure S13. Fitting of the experimental data obtained from the titrations of *Z*-5AUP with DAP.

The fitting results are well consistent and the mean value of the association constant is K_Z= 4040 ± 355 M^{-1}. (Table S20)

Table S20. Fitting data for the three titration experiments.

	K (M^{-1})	Sd	δ_{max}	sd	K_{mean} (M^{-1})	sd
Z1	3960	330	11.914	0.043		
Z2	3650	350	11.986	0.063		
Z3	4510	280	11.895	0.066	4040	355

Titration of Upr.

Two independent titration experiments have been made in toluene-d_8 at 25 °C. (Table S21)

Table S21. Conditions employed in two different titration experiments of Upr complexation upon DAP addition.

	[Upr] (M)	[DAP] range (M)
UPR1	0.00334	0 – 0.009
UPR2	0.00308	0 – 0.009

Also in this case better fitting are obtained optimizing the concentration of Upr as a parameter, (Figure S14) with differences between the nominal and the calculated concentration below 15%.

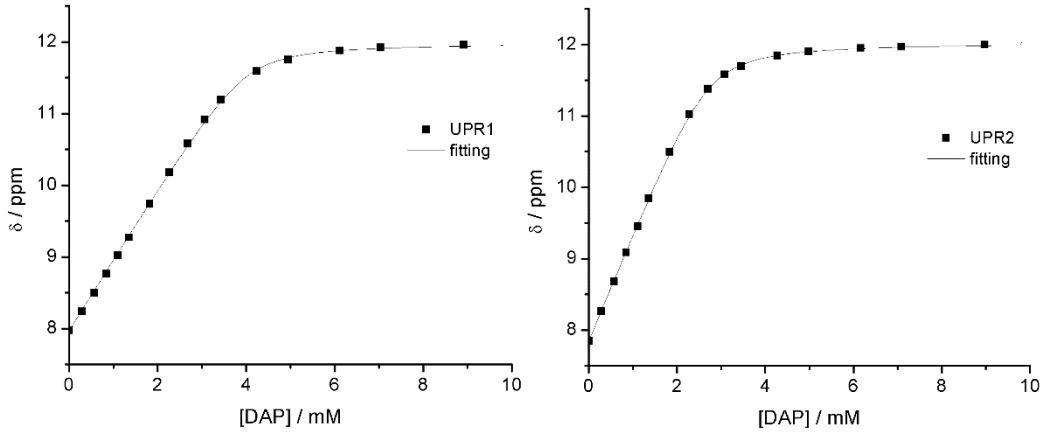

Figure S14. Fitting of the titration experiments UPR1 and UPR2.

The data obtained from the fittings are summarized in Table S22.

Table S22: Fitting data for the two titration experiments.

	K (M^{-1})	sd	δ_{max}	sd	[Upr] (M)	Sd
UPR1	15200	2700	11.993	0.025	0.003997	3.20E-05
UPR2	12730	850	12.036	0.011	0.002716	1.60E-05

The mean value of the association constant is K_E= 13965 ± 1235 M^{-1}.

DFT calculation of gas-phase models.

Our theoretical calculations are based on DFT using PWSCF code of the Quantum ESPRESSO distribution.[3] The Van der Waals density functional (VdW-DF)[6][7][8] was used in conjunction with a GGA-PBE functional[5] to describe the system. The optimization of the gas-phase models for the isolated DAP, *cis*-5AUP, *trans*-5AUP molecules and for the *cis*- and *trans*-5AUP·DAP molecular complexes confirms the higher stability of the *trans* isomers relative to their *cis* counterparts (by 0.65 eV for isolated 5AUP, and 0.61 eV for 5AUP·DAP). The fully relaxed optimized structures for ***Z*-5UAP·DAP** is shown in Fig 15, the relaxed coordinates for the ***Z*-5AUP** and ***Z*-5UAP·DAP** structures are also provided below in xyz format in the tables below.

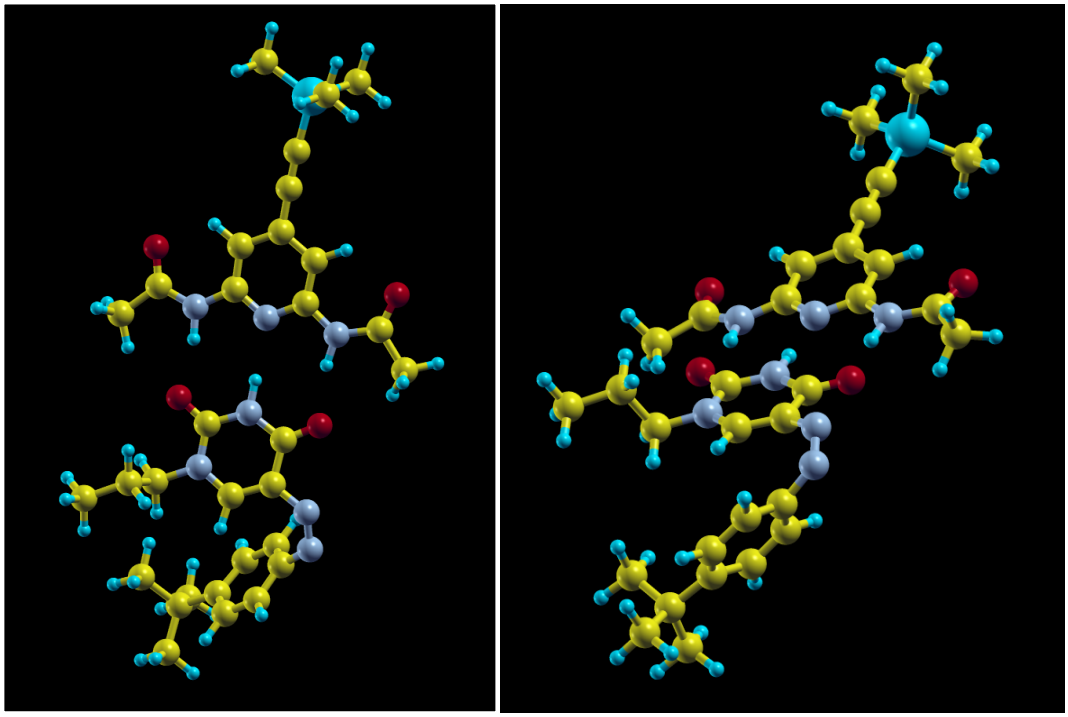

Figure 15. Fully relaxed computed structure for *Z*-5UAP·DAP, shown from two different angles.

***Z*-5AUP** (45 atoms, A units)**:**

C	10.195227	11.845826	11.268832
C	10.547063	13.264862	11.224607
C	8.126406	13.779071	10.974013
C	8.875200	11.493177	11.158136
H	8.546007	10.459404	11.195879
C	6.460382	11.948614	10.797672
H	6.517720	10.949809	10.344920
H	5.999752	12.628442	10.068101
C	5.635331	11.915107	12.094325
H	5.607506	12.927651	12.526072
H	6.139242	11.260294	12.824842
C	4.205553	11.410225	11.831030
H	3.674828	12.070628	11.128767
H	3.626061	11.376792	12.763010
H	4.211288	10.395887	11.402361
C	10.467832	9.299510	10.143195

C	9.694864	8.182258	10.475169
H	9.851420	7.692018	11.436947
C	8.683113	7.755710	9.611144
H	8.066026	6.917227	9.927867
C	8.449074	8.387302	8.374378
C	9.324891	9.433977	8.015814
H	9.225376	9.927824	7.050557
C	10.318712	9.892655	8.881795
H	10.954827	10.732315	8.595625
C	7.234036	8.009340	7.492432
C	6.829550	6.521229	7.674577
H	6.469928	6.307629	8.690238
H	7.673639	5.850109	7.458936
H	6.010897	6.274069	6.984094
C	6.034991	8.910320	7.926234
H	6.273572	9.976233	7.789219
H	5.785260	8.745698	8.985740
H	5.141900	8.679622	7.325742
C	7.517518	8.246933	5.984413
H	7.667744	9.309435	5.750118
H	6.659732	7.902993	5.389230
H	8.407425	7.691053	5.655018
N	11.391446	9.793226	11.132188
N	11.280582	10.964625	11.593946
N	9.452437	14.130361	11.092548
H	9.653254	15.155994	11.053740
N	7.861599	12.405525	10.997447
O	11.698163	13.721257	11.269647
O	7.223972	14.617963	10.845340

***Z*-5UAP·DAP** (84 atoms, A units)**:**

C	10.195227	11.845826	11.268832
C	10.547063	13.264862	11.224607

C	8.126406	13.779071	10.974013
C	8.875200	11.493177	11.158136
H	8.546007	10.459404	11.195879
C	6.460382	11.948614	10.797672
H	6.517720	10.949809	10.344920
H	5.999752	12.628442	10.068101
C	5.635331	11.915107	12.094325
H	5.607506	12.927651	12.526072
H	6.139242	11.260294	12.824842
C	4.205553	11.410225	11.831030
H	3.674828	12.070628	11.128767
H	3.626061	11.376792	12.763010
H	4.211288	10.395887	11.402361
C	10.467832	9.299510	10.143195
C	9.694864	8.182258	10.475169
H	9.851420	7.692018	11.436947
C	8.683113	7.755710	9.611144
H	8.066026	6.917227	9.927867
C	8.449074	8.387302	8.374378
C	9.324891	9.433977	8.015814
H	9.225376	9.927824	7.050557

C	10.318712	9.892655	8.881795
H	10.954827	10.732315	8.595625
C	7.234036	8.009340	7.492432
C	6.829550	6.521229	7.674577
H	6.469928	6.307629	8.690238
H	7.673639	5.850109	7.458936
H	6.010897	6.274069	6.984094
C	6.034991	8.910320	7.926234
H	6.273572	9.976233	7.789219
H	5.785260	8.745698	8.985740
H	5.141900	8.679622	7.325742
C	7.517518	8.246933	5.984413
H	7.667744	9.309435	5.750118
H	6.659732	7.902993	5.389230
H	8.407425	7.691053	5.655018
N	11.391446	9.793226	11.132188
N	11.280582	10.964625	11.593946
N	9.452437	14.130361	11.092548
H	9.653254	15.155994	11.053740
N	7.861599	12.405525	10.997447
O	11.698163	13.721257	11.269647

O	7.223972	14.617963	10.845340
C	11.253690	17.608170	11.312216
C	11.536444	18.966494	11.513745
H	12.543138	19.293780	11.737787
C	10.478107	19.883535	11.420309
C	9.186008	19.430986	11.108628
H	8.356554	20.119917	11.016590
C	9.001632	18.054336	10.919269
C	6.583785	18.163570	10.260512
C	5.377688	17.281218	9.946116
H	4.617923	17.450448	10.724224
H	5.601175	16.209544	9.890537
H	4.949367	17.624553	8.994345
C	13.608766	16.773843	11.579729
C	14.397791	15.471515	11.666815
H	15.446344	15.692038	11.438601
H	14.015063	14.689468	10.998968
H	14.337917	15.082735	12.696499
C	10.727161	21.266449	11.656306
C	10.974552	22.443532	11.885602
C	12.906689	24.649653	11.191346

H	13.762087	23.985129	11.385159
H	13.229522	25.685168	11.381776
H	12.650606	24.563756	10.124839
C	9.950921	25.297733	11.934186
H	9.658880	25.247963	10.874595
H	10.179222	26.347797	12.175116
H	9.081644	24.992624	12.535820
C	11.911028	24.242557	14.109826
H	11.060912	23.959541	14.748374
H	12.234709	25.253712	14.402473
H	12.736384	23.546399	14.321516
N	7.750002	17.493611	10.601554
H	7.697453	16.471780	10.627735
N	10.006819	17.148809	11.031478
N	12.239781	16.611481	11.389000
H	11.917760	15.643448	11.284543
O	6.499777	19.393784	10.209704
O	14.152171	17.876746	11.694938
Si	11.43554	1 24.18338	12.28128

References

[1] G. M. Sheldrick, *Acta Crystallogr. Sect. A Found. Crystallogr.* **2007**, *64*, 112–122.

[2] P. Kuzmic, *Anal. Biochem.* **1996**, *237*, 260–273.

[3] P. Giannozzi, S. Baroni, N. Bonini, M. Calandra, R. Car, C. Cavazzoni, D. Ceresoli, G. L. Chiarotti, M. Cococcioni, I. Dabo, A. Dal Corso, S. de Gironcoli, S. Fabris, G. Fratesi, R. Gebauer, U. Gerstmann, C. Gougoussis, A. Kokalj, M. Lazzeri, L. Martin-Samos, N. Marzari, F. Mauri, R. Mazzarello, S. Paolini, A. Pasquarello, L. Paulatto, C. Sbraccia, S. Scandolo, G. Sclauzero, A. P. Seitsonen, A. Smogunov, P. Umari, R. M. Wentzcovitch, *J. Phys. Condens. Matter* **2009**, *21*, 395502.

[4] D. Vanderbilt, *Phys. Rev. B* **1990**, *41*, 7892–7895.

[5] J. P. Perdew, K. Burke, M. Ernzerhof, *Phys. Rev. Lett.* **1996**, *77*, 3865–3868.

[6] T. Thonhauser, V. R. Cooper, S. Li, A. Puzder, P. Hyldgaard, D. C. Langreth, *Phys. Rev. B* **2007**, *76*, 125112.

[7] M. Dion, H. Rydberg, E. Schröder, D. C. Langreth, B. I. Lundqvist, *Phys. Rev. Lett.* **2004**, *92*, 246401.

[8] D. C. Langreth, B. I. Lundqvist, S. D. Chakarova-Käck, V. R. Cooper, M. Dion, P. Hyldgaard, a Kelkkanen, J. Kleis, L. Kong, S. Li, P. G. Moses, E. Murray, A. Puzder, H. Rydberg, E. Schroeder, T. Thonhauser, *J. Phys. Condens. Matter* **2009**, *21*, 84203.

[9] G. Román-Pérez, J. M. Soler, *Phys. Rev. Lett.* **2009**, *103*, 96102.

[10] A. Kokalj, *Comput. Mater. Sci.* **2003**, *28*, 155–168.

[11] A. Llanes-Pallas, C. Palma, L. Piot, A. Belbakra, A. Listorti, M. Prato, P. Samori, N. Armaroli, D. Bonifazi, *J. Am. Chem. Soc.* **2009**, *131*, 509–520.

[12] J. M. Wilson, G. Henderson, F. Black, A. Sutherland, R. L. Ludwig, K. H. Vousden, D. J. Robins, *Bioorg. Med. Chem.* **2007**, *15*, 77–86.

[13] M. P. Doyle, W. J. Bryker, *J. Org. Chem.* **1979**, *44*, 1572–1574.

[14] P. N. Juri, R. A. Bartsch, *J. Org. Chem.* **1980**, *45*, 2028–2030.

[15] C. G. Swain, R. J. Rogers, *J. Am. Chem. Soc.* **1975**, *97*, 799–800.

[16] F. Kopp, P. Knochel, *Org. Lett.* **2007**, *9*, 1639–1641.

[17] J. P. Horwitz, A. J. Tomson, *J. Org. Chem.* **1961**, *26*, 3392–3395.

[18] D. N. Abrams, Y. W. Lee, E. E. Knaus, L. I. Wiebe, *Int. J. Appl. Radiat. Isot.* **1984**, *35*, 531–535.

[19] D. T. Browne, J. Eisinger, N. J. Leonard, *J. Am. Chem. Soc.* **1968**, *90*, 7302–7323.